

$b \rightarrow s$ Transitions in Family-dependent $U(1)'$ Models

Vernon Barger^a, Lisa L. Everett^a, Jing Jiang^a, Paul Langacker^b,
Tao Liu^c and Carlos E.M. Wagner^{c,d,e}

^aDepartment of Physics, University of Wisconsin, Madison, WI 53706

^bSchool of Natural Science, Institute for Advanced Study,
Einstein Drive, Princeton, NJ 08540

^cEnrico Fermi Institute and ^dKavli Institute for Cosmological Physics,
University of Chicago, 5640 S. Ellis Ave., Chicago, IL 60637

^eHEP Division, Argonne National Laboratory, 9700 Cass Ave., Argonne, IL 60439

Abstract

We analyze flavor-changing-neutral-current (FCNC) effects in the $b \rightarrow s$ transitions that are induced by family non-universal $U(1)'$ gauge symmetries. After systematically developing the necessary formalism, we present a correlated analysis for the $\Delta B = 1, 2$ processes. We adopt a model-independent approach in which we only require family-universal charges for the first and second generations and small fermion mixing angles. We analyze the constraints on the resulting parameter space from $B_s - \bar{B}_s$ mixing and the time-dependent CP asymmetries of the penguin-dominated $B_d \rightarrow (\pi, \phi, \eta', \rho, \omega, f_0)K_S$ decays. Our results indicate that the currently observed discrepancies in some of these modes with respect to the Standard Model predictions can be consistently accommodated within this general class of models.

1 Introduction

The origin of CP violation, which was first observed in the kaon system four decades ago [1], has remained one of the fundamental questions of elementary particle physics. In recent years, the B factories have established that the Standard Model (SM) picture of CP violation, in which all CP -violating effects are generated by the single phase δ_{CKM} in the Cabibbo-Kobayashi-Maskawa (CKM) quark mixing matrix [2, 3], is consistent with the observed pattern of CP -violating phenomena in both the B_d and K meson systems [4]. However, as the SM cannot account for the baryon asymmetry in the Universe today [5], new physics (NP) is *necessarily* required to describe all observed phenomena with CP -violation involved.

One arena to seek the NP effects is in flavor-changing neutral current transitions (FCNC) where the SM contributions first appear at the one-loop level and the NP effects can be competitive. The emblematic set of such processes is the set of $b \rightarrow s$ transitions, which include $B_s - \bar{B}_s$ mixing and the set of neutral B_d meson decays which occur via $b \rightarrow s\bar{q}q$ ($q = u, d, c, s$) transitions. Several of these processes are also of interest because recent measurements exhibit discrepancies with the SM predictions at the level of a few standard deviations, which may suggest the intriguing possibility of physics beyond the SM. The current status of the data is as follows:

- **$B_s - \bar{B}_s$ mixing phase.** The standard way to parametrize NP in $B_s - \bar{B}_s$ mixing is to express the off-diagonal mixing matrix element as follows:

$$M_{12}^{B_s} = (M_{12}^{B_s})_{\text{SM}} C_{B_s} e^{2i\phi_{B_s}^{\text{NP}}}. \quad (1.1)$$

The SM predicts that $C_{B_s} = 1$ and $\phi_{B_s}^{\text{NP}} = 0$. Though the data indicate that C_{B_s} does not differ significantly from unity, the results of a recent analysis [6] suggest that $\phi_{B_s}^{\text{NP}}$ deviates from zero at the 3σ level (see Table 1). This analysis combines all the available experimental results on B_s mixing, including the new tagged analyses of $B_s \rightarrow \psi\phi$ by CDF [7] and DØ [8] (note that no single measurement yet has a 3σ significance.). The discrepancy disfavors NP scenarios which obey minimal flavor violation (MFV), *i.e.*, with $\phi_{B_s}^{\text{NP}} \approx 0$, and instead suggests NP which exhibits flavor violation in the $b \rightarrow s$ transitions (e.g., see [9] and references therein). For convenience, in Table 1 we also give the data in terms of $A_s^{\text{NP}}/A_s^{\text{SM}}$ and ϕ_s^{NP} which are related to C_{B_s} and $\phi_{B_s}^{\text{NP}}$ according to

$$C_{B_s} e^{2i\phi_{B_s}^{\text{NP}}} = 1 + \frac{A_s^{\text{NP}}}{A_s^{\text{SM}}} e^{2i\phi_s^{\text{NP}}}. \quad (1.2)$$

- **CP asymmetries in neutral B_d decays.** The set of neutral B_d decays in question is the set of QCD penguin-dominated charmless decays that occur via $b \rightarrow s\bar{q}q$ ($q = u, d, c, s$) transitions. The CP asymmetries of such decays into a final CP -eigenstate f_{CP} are given by

$$\mathcal{A}_{f_{CP}}(t) = \left. \frac{\Gamma(\bar{B}_d(t) \rightarrow f_{CP}) - \Gamma(B_d(t) \rightarrow f_{CP})}{\Gamma(\bar{B}_d(t) \rightarrow f_{CP}) + \Gamma(B_d(t) \rightarrow f_{CP})} \right|_{\Delta\Gamma_{B_d}=0}$$

Observable	1 σ C.L.	2 σ C.L.
$\phi_{B_s}^{\text{NP}} [^\circ]$ (S1)	-20.3 ± 5.3	$[-30.5, -9.9]$
$\phi_{B_s}^{\text{NP}} [^\circ]$ (S2)	-68.0 ± 4.8	$[-77.8, -58.2]$
C_{B_s}	1.00 ± 0.20	$[0.68, 1.51]$
$\phi_s^{\text{NP}} [^\circ]$ (S1)	-56.3 ± 8.3	$[-69.8, -36.0]$
$A_s^{\text{NP}}/A_s^{\text{SM}}$ (S1)	0.66 ± 0.28	$[0.24, 1.11]$
$\phi_s^{\text{NP}} [^\circ]$ (S2)	-79.1 ± 2.6	$[-84.0, -72.8]$
$A_s^{\text{NP}}/A_s^{\text{SM}}$ (S2)	1.78 ± 0.03	$[1.53, 2.19]$

Table 1: Fit results for the $B_s - \bar{B}_s$ mixing parameters [6]. The two $\phi_{B_s}^{\text{NP}}$ solutions (“S1” and “S2”) result from measurement ambiguities; see [6] for details.

$$= -\mathcal{C}_{f_{CP}} \cos(\Delta M_{B_d} t) + \mathcal{S}_{f_{CP}} \sin(\Delta M_{B_d} t), \quad (1.3)$$

in which $\mathcal{C}_{f_{CP}}$ and $\mathcal{S}_{f_{CP}}$ are direct and mixing-induced CP asymmetry parameters. The SM predictions for many decays of this type, including $B_d \rightarrow \psi K_S$ and $B_d \rightarrow (\phi, \eta', \pi, \rho, \omega, f_0) K_S$ are as follows:

$$-\eta_{f_{CP}} \mathcal{S}_{f_{CP}} = \sin 2\beta + \mathcal{O}(\lambda^2), \quad \mathcal{C}_{f_{CP}} = 0 + \mathcal{O}(\lambda^2), \quad (1.4)$$

with $\beta \equiv \arg[-(V_{cd}V_{cb}^*)/(V_{td}V_{tb}^*)]$, $\lambda = \sin \theta_c$ being the Cabibbo angle, and $\eta_{f_{CP}} = \pm 1$ being the CP eigenvalue for the final state f_{CP} . However, the central values of $\sin 2\beta$ directly measured from the penguin-dominated modes are systematically below the SM prediction and the results obtained from measuring the charmed $B_d \rightarrow \psi K_S$ mode. Meanwhile, the central values of the direct CP asymmetry measured from $B_d \rightarrow \phi K_S$ and $B_d \rightarrow \omega K_S$ modes are also small compared to that obtained from the $B_d \rightarrow \psi K_S$ mode (see Table 2). Given that the $B_d \rightarrow \psi K_S$ decay is dominated by tree-level amplitude in the SM, large absolute values for $\Delta \mathcal{S}_{f_{CP}} = -\eta_{f_{CP}} \mathcal{S}_{f_{CP}} + \eta_{\psi K_S} \mathcal{S}_{\psi K_S}$ and $\Delta \mathcal{C}_{f_{CP}} = \mathcal{C}_{f_{CP}} - \mathcal{C}_{\psi K_S}$ may imply interesting NP in the $b \rightarrow s$ transitions. .

To account for these discrepancies appearing in $B_s - \bar{B}_s$ mixing and B_d decays, a number of NP scenarios have been studied, including low energy supersymmetry and models with warped extra dimensions, among others [11]. In many of these scenarios, the effects of NP in the $b \rightarrow s$ transitions are loop-suppressed and can compete with SM contributions. The most popular and well-studied scenarios are models with minimal flavor violation (MFV), in which the only source of CP violation is the single irremovable phase of the Cabibbo-Kobayashi-Maskawa mixing matrix. MFV scenarios, however, face difficulties in that they do not generally allow for a nonvanishing ϕ_{B_s} .

f_{CP}	$-\eta_{CP}\mathcal{S}_{f_{CP}} (1\sigma \text{ C.L.})$	$\mathcal{C}_{f_{CP}}(1\sigma \text{ C.L.})$
ψK_S	$+0.672 \pm 0.024$	$+0.005 \pm 0.019$
ϕK_S	$+0.44^{+0.17}_{-0.18}$	-0.23 ± 0.15
$\eta' K_S$	$+0.59 \pm 0.07$	-0.05 ± 0.05
πK_S	$+0.57 \pm 0.17$	$+0.01 \pm 0.10$
ρK_S	$+0.63^{+0.17}_{-0.21}$	-0.01 ± 0.20
ωK_S	$+0.45 \pm 0.24$	-0.32 ± 0.17
$f_0 K_S$	$+0.62^{+0.11}_{-0.13}$	0.10 ± 0.13

Table 2: World averages of the experimental results for the CP asymmetries in B_d decays via $b \rightarrow \bar{q}qs$ transitions [10].

In this work, we will study the constraints from $b \rightarrow s$ transitions on models with family non-universal gauged $U(1)'$ symmetries. Additional $U(1)'$ gauge symmetries are present in many well-motivated extensions of the SM, such as grand unified and/or string models (e.g., see [12] for a review). Such scenarios are of particular interest because unlike the scenarios studied above, they allow for the intriguing possibility of *tree-level* FCNC, with contributions that are competitive with the SM even for small $U(1)'$ couplings. Depending on the details of the model, family-dependent $U(1)'$ scenarios can result in new FC operators and/or modified Wilson coefficients to the existing SM operators in the operator product expansion, providing a rich framework beyond MFV to explore FCNC and CP -violating effects.

We follow the general framework for addressing Z' -induced FCNC as developed in [13] and systemize its application to $b \rightarrow s$ transitions. Rather than considering specific $U(1)'$ models, we adopt a model-independent approach in which the main restrictions are family universal charges for the first and second generations and small fermion mixing angles. We also neglect the effects of $Z - Z'$ mixing (which are known to be small), and assume the absence of any exotic fermions that could mix with the usual SM fermions through non-universal Z' couplings, which may also result in nontrivial FCNC effects (e.g., see [12]).

This work is an extension of our earlier work [14, 16], in which we performed a *correlated* analysis of the $\Delta B = 1, 2$ processes mentioned above for a specific set of $U(1)'$ scenarios. That analysis was in contrast to other studies of $U(1)'$ scenarios based on mode-by-mode analyses [15]. The purpose of this paper is twofold: first, to provide more details of the formalism and analysis than were given explicitly in [14], and sec-

ond, to analyze a more general set of $U(1)'$ models. Our results demonstrate that the $b \rightarrow s$ transitions not only place important constraints on family non-universal Z' couplings and mass scale, but also that family non-universal $U(1)'$ scenarios can explain the currently observed discrepancies with the SM predictions for $B_s - \bar{B}_s$ mixing and the time-dependent CP asymmetries of the penguin-dominated $B_d \rightarrow (\pi, \phi, \eta', \rho, \omega, f_0)K_S$ decays.

This paper is structured as follows. We begin by providing an overview of the formalism of the Z' induced FCNC effects in the $b \rightarrow s$ transitions and present the effective Hamiltonian for the processes of interest at the b quark mass scale in Section 2. In Section 3, first we analyze the FCNC constraints within several special limits of the general $U(1)'$ parameter space, and then turn to a more general analysis. Our summary and conclusions are presented in Section 4.

2 Theoretical Background

2.1 Formalism of Z' -induced FCNC Effects

The general framework for studying Z' -induced FCNC Effects has been developed in [13]. In this section, we will systematically formalize its applications to the case of the $b \rightarrow s$ transitions (the generalization to $b \rightarrow d$ transitions is straightforward).

We begin by considering the SM extended by a single additional $U(1)'$ gauge symmetry (the generalization to multiple $U(1)'$ gauge symmetries is straightforward). In this theory, the neutral current Lagrangian in the SM gauge eigenstate basis is given by

$$\mathcal{L}_{NC} = -eJ_{\text{em}}^\mu A_\mu - g_1 J_Z^\mu Z_\mu - g_2 J_{Z'}^\mu Z'_\mu, \quad (2.5)$$

in which A_μ is the $U(1)_{\text{em}}$ gauge boson, Z_μ is the massive electroweak (EW) neutral gauge boson, Z'_μ is the gauge boson associated with the additional Abelian gauge symmetry, and $g_1 = g/\cos\theta_W$ and g_2 are the gauge couplings of the Z_μ and Z'_μ bosons, respectively. The currents are given by

$$J_Z^\mu = \sum_\psi \sum_i \bar{\psi}_i \gamma^\mu \left[\epsilon_i^{\psi L} P_L + \epsilon_i^{\psi R} P_R \right] \psi_i, \quad (2.6)$$

$$J_{Z'}^\mu = \sum_\psi \sum_{i,j} \bar{\psi}_i \gamma^\mu \left[\tilde{\epsilon}_{ij}^{\psi L} P_L + \tilde{\epsilon}_{ij}^{\psi R} P_R \right] \psi_j, \quad (2.7)$$

in which ψ labels the SM fermions, i and j are family indices, and $P_{R,L} = (1 \pm \gamma_5)/2$. The (family universal) SM chiral charges are given by

$$\epsilon_i^{\psi L} = t_3^{\psi L} - \sin^2\theta_W Q_{\psi L}, \quad \epsilon_i^{\psi R} = -\sin^2\theta_W Q_{\psi R}, \quad (2.8)$$

in which $t_3^{\psi L}$ denotes the third component of the weak isospin and $Q_{\psi_{L,R}}$ are the electric charges of $\psi_{L,R}$. Without loss of generality, the Z' chiral charges can be diagonalized by choosing the appropriate gauge basis for the fermions:

$$\tilde{\epsilon}_{ij}^{\psi_{L,R}} = \tilde{\epsilon}_i^{\psi_{L,R}} \delta_{ij}. \quad (2.9)$$

In particular, $SU(2)_L$ symmetry requires that

$$\tilde{\epsilon}_i^{u_L} \equiv \tilde{\epsilon}_i^{d_L}, \quad \tilde{\epsilon}_i^{e_L} \equiv \tilde{\epsilon}_i^{\nu_L}. \quad (2.10)$$

If the diagonal $U(1)'$ chiral charges are non-universal, flavor-changing (FC) Z' couplings are generically induced by fermion mixing. The fermion Yukawa matrices h_ψ in the weak eigenstate basis are diagonalized by the unitary matrices $V_{\psi_{L,R}}$, such that

$$h_{\psi,diag} = V_{\psi_R} h_\psi V_{\psi_L}^\dagger, \quad (2.11)$$

and the CKM matrix is given by

$$V_{\text{CKM}} = V_{u_L} V_{d_L}^\dagger. \quad (2.12)$$

Hence, the chiral Z' couplings in the fermion mass eigenstate basis take the form:

$$B^{\psi_L} \equiv V_{\psi_L} \tilde{\epsilon}^{\psi_L} V_{\psi_L}^\dagger, \quad B^{\psi_R} \equiv V_{\psi_R} \tilde{\epsilon}^{\psi_R} V_{\psi_R}^\dagger. \quad (2.13)$$

However, it is known that the constraints from $K - \bar{K}$ mixing and from $\mu - e$ conversion in muonic atoms exclude significant non-universal effects for the first two families, which suggests that

$$B^{\psi_{L,R}} = \begin{pmatrix} B_{11}^{\psi_{L,R}} & 0 & B_{13}^{\psi_{L,R}} \\ 0 & B_{11}^{\psi_{L,R}} & B_{23}^{\psi_{L,R}} \\ B_{13}^{\psi_{L,R}*} & B_{23}^{\psi_{L,R}*} & B_{33}^{\psi_{L,R}} \end{pmatrix}, \quad (2.14)$$

at least for the down-type quarks and e, μ, τ leptons. The most straightforward way to achieve this coupling structure is to assume universal $U(1)'$ charges for the down-type fermions of the first two families, *i.e.*,

$$\tilde{\epsilon}^{\psi_{L,R}} = \begin{pmatrix} \tilde{\epsilon}_1^{\psi_{L,R}} & 0 & 0 \\ 0 & \tilde{\epsilon}_1^{\psi_{L,R}} & 0 \\ 0 & 0 & \tilde{\epsilon}_3^{\psi_{L,R}} \end{pmatrix}. \quad (2.15)$$

With the unitary matrices $V_{\psi_{L,R}}$ written as

$$V_{\psi_{L,R}} = \begin{pmatrix} W_{\psi_{L,R}} & X_{\psi_{L,R}} \\ Y_{\psi_{L,R}} & Z_{\psi_{L,R}} \end{pmatrix}, \quad (2.16)$$

where $W_{\psi_{L,R}}$ is a 2×2 submatrix, one obtains

$$B^{\psi_{L,R}} = \begin{pmatrix} \tilde{\epsilon}_1^{\psi_{L,R}} W_{\psi_{L,R}}^\dagger W_{\psi_{L,R}} + \tilde{\epsilon}_3^{\psi_{L,R}} Y_{\psi_{L,R}}^\dagger Y_{\psi_{L,R}} & \tilde{\epsilon}_1^{\psi_{L,R}} W_{\psi_{L,R}}^\dagger X_{\psi_{L,R}} + \tilde{\epsilon}_3^{\psi_{L,R}} Y_{\psi_{L,R}}^\dagger Z_{\psi_{L,R}} \\ \tilde{\epsilon}_1^{\psi_{L,R}} X_{\psi_{L,R}}^\dagger W_{\psi_{L,R}} + \tilde{\epsilon}_3^{\psi_{L,R}} Z_{\psi_{L,R}}^\dagger Y_{\psi_{L,R}} & \tilde{\epsilon}_1^{\psi_{L,R}} X_{\psi_{L,R}}^\dagger X_{\psi_{L,R}} + \tilde{\epsilon}_3^{\psi_{L,R}} Z_{\psi_{L,R}}^\dagger Z_{\psi_{L,R}} \end{pmatrix}. \quad (2.17)$$

Therefore, in the limit of small fermion mixing angles or small $X_{\psi_{L,R}}, Y_{\psi_{L,R}}$ elements, a Z' coupling structure of the type given in Eq. (2.14) is produced, in which

$$\begin{aligned} B_{11}^{\psi_{L,R}} &= \tilde{\epsilon}_1^{\psi_{L,R}}, & B_{33}^{\psi_{L,R}} &= \tilde{\epsilon}_3^{\psi_{L,R}} \\ B_{13}^{\psi_{L,R}}, B_{23}^{\psi_{L,R}} &\sim \mathcal{O}(X_{\psi_{L,R}}, Y_{\psi_{L,R}}), \end{aligned} \quad (2.18)$$

such that $B_{13}^{\psi_{L,R}}$ and $B_{23}^{\psi_{L,R}}$ are in general both complex parameters.

EW symmetry breaking induces $Z - Z'$ mixing, such that the gauge eigenstates Z_μ and Z'_μ are related to the mass eigenstates $Z_\mu^{(n)}$ ($n = 1, 2$) by an orthogonal transformation. In the mass eigenstate basis, the Lagrangian couplings are given by

$$\mathcal{L}_{NC}^Z = - [g_1 \cos \theta J_Z^\mu + g_2 \sin \theta J_{Z'}^\mu] Z_\mu^{(1)} - [-g_1 \sin \theta J_Z^\mu + g_2 \cos \theta J_{Z'}^\mu] Z_\mu^{(2)}, \quad (2.19)$$

where θ is the $Z - Z'$ mixing angle, J_Z^μ is given in Eq. (2.6), and $J_{Z'}^\mu$ is of the form of Eq. (2.7) with $\tilde{\epsilon}^{\psi_{L,R}}$ replaced by $B^{\psi_{L,R}}$ from Eq. (2.13). In this analysis, we neglect kinetic mixing since it simply amounts to a redefinition of the unknown Z' couplings.¹

At the EW scale, the tree-level four-fermion interactions are described by the product of gauge currents

$$\begin{aligned} \mathcal{L}_{eff} &= \frac{-4G_F}{\sqrt{2}} (\rho_{eff} J_Z^2 + 2w J_Z \cdot J_{Z'} + y J_{Z'}^2) \\ &= \frac{-4G_F}{\sqrt{2}} \sum_{\psi, \chi} \sum_{i, j, m, n} \left[C_{mn}^{ij} S_{mn}^{ij} + \tilde{C}_{mn}^{ij} \tilde{S}_{mn}^{ij} + D_{mn}^{ij} T_{mn}^{ij} + \tilde{D}_{mn}^{ij} \tilde{T}_{mn}^{ij} \right]. \end{aligned} \quad (2.20)$$

In Eq. (2.20), the local current-current operators are² (i, j, m, n are family indices):

$$\begin{aligned} S_{mn}^{ij} &= (\bar{\psi}_i \gamma^\mu P_L \psi_j) (\bar{\chi}_m \gamma_\mu P_L \chi_n), & \tilde{S}_{mn}^{ij} &= (\bar{\psi}_i \gamma^\mu P_R \psi_j) (\bar{\chi}_m \gamma_\mu P_R \chi_n), \\ T_{mn}^{ij} &= (\bar{\psi}_i \gamma^\mu P_L \psi_j) (\bar{\chi}_m \gamma_\mu P_R \chi_n), & \tilde{T}_{mn}^{ij} &= (\bar{\psi}_i \gamma^\mu P_R \psi_j) (\bar{\chi}_m \gamma_\mu P_L \chi_n), \end{aligned} \quad (2.21)$$

and the coefficients are

$$\begin{aligned} C_{mn}^{ij} &= \rho_{eff} \delta_{ij} \delta_{mn} \epsilon_i^{\psi_L} \epsilon_m^{\chi_L} + w \delta_{ij} \epsilon_i^{\psi_L} B_{mn}^{\chi_L} + w \delta_{mn} \epsilon_m^{\chi_L} B_{ij}^{\psi_L} + y B_{ij}^{\psi_L} B_{mn}^{\chi_L}, \\ \tilde{C}_{mn}^{ij} &= \rho_{eff} \delta_{ij} \delta_{mn} \epsilon_i^{\psi_R} \epsilon_m^{\chi_R} + w \delta_{ij} \epsilon_i^{\psi_R} B_{mn}^{\chi_R} + w \delta_{mn} \epsilon_m^{\chi_R} B_{ij}^{\psi_R} + y B_{ij}^{\psi_R} B_{mn}^{\chi_R}, \\ D_{mn}^{ij} &= \rho_{eff} \delta_{ij} \delta_{mn} \epsilon_i^{\psi_L} \epsilon_m^{\chi_R} + w \delta_{ij} \epsilon_i^{\psi_L} B_{mn}^{\chi_R} + w \delta_{mn} \epsilon_m^{\chi_R} B_{ij}^{\psi_L} + y B_{ij}^{\psi_L} B_{mn}^{\chi_R}, \\ \tilde{D}_{mn}^{ij} &= \rho_{eff} \delta_{ij} \delta_{mn} \epsilon_i^{\psi_R} \epsilon_m^{\chi_L} + w \delta_{ij} \epsilon_i^{\psi_R} B_{mn}^{\chi_L} + w \delta_{mn} \epsilon_m^{\chi_L} B_{ij}^{\psi_R} + y B_{ij}^{\psi_R} B_{mn}^{\chi_L}, \end{aligned} \quad (2.22)$$

¹Kinetic mixing allows the redefined Z' charges to have a component of weak hypercharge, which would otherwise not be allowed. This feature is irrelevant for the purposes of this paper.

²These operators are not all independent. For couplings of four fermions of the same type, $\psi = \chi$, e.g. four charged leptons, one has $S_{mn}^{ij} = S_{ij}^{mn}$, $\tilde{S}_{mn}^{ij} = \tilde{S}_{ij}^{mn}$ and $T_{mn}^{ij} = \tilde{T}_{ij}^{mn}$.

in which

$$\begin{aligned}
\rho_{eff} &= \rho_1 \cos^2 \theta + \rho_2 \sin^2 \theta, & \rho_a &= \frac{M_W^2}{M_a^2 \cos^2 \theta_W}, \\
w &= \frac{g_2}{g_1} \sin \theta \cos \theta (\rho_1 - \rho_2), \\
y &= \left(\frac{g_2}{g_1} \right)^2 (\rho_1 \sin^2 \theta + \rho_2 \cos^2 \theta).
\end{aligned} \tag{2.23}$$

In Eqs. (2.23), M_a denotes the masses of the neutral gauge boson mass eigenstates, and θ_W is the EW mixing angle. We do not specify the ψ and χ dependence of the coefficients $C, \tilde{C}, D, \tilde{D}$ in Eqs. (2.22), which can be understood from the context.

For $b \rightarrow s$ transitions, the local operators are given by $S_{mn}^{bs}, \tilde{S}_{mn}^{bs}, T_{mn}^{bs}$ and \tilde{T}_{mn}^{bs} , with coefficients that are given by

$$\begin{aligned}
C_{mn}^{bs} &= w \delta_{mn} \epsilon_m^{\chi L} B_{bs}^L + y B_{bs}^L B_{mn}^{\chi L}, \\
\tilde{C}_{mn}^{bs} &= w \delta_{mn} \epsilon_m^{\chi R} B_{bs}^R + y B_{bs}^R B_{mn}^{\chi R}, \\
D_{mn}^{bs} &= w \delta_{mn} \epsilon_m^{\chi R} B_{bs}^L + y B_{bs}^L B_{mn}^{\chi R}, \\
\tilde{D}_{mn}^{bs} &= w \delta_{mn} \epsilon_m^{\chi R} B_{bs}^R + y B_{bs}^R B_{mn}^{\chi L}.
\end{aligned} \tag{2.24}$$

With the $Z - Z'$ mixing angle neglected, the coefficients can be written as

$$\begin{aligned}
C_{mn}^{bs} &= \left(\frac{g_2 M_Z}{g_1 M_{Z'}} \right)^2 B_{bs}^L B_{mn}^{\chi L}, \\
\tilde{C}_{mn}^{bs} &= \left(\frac{g_2 M_Z}{g_1 M_{Z'}} \right)^2 B_{bs}^R B_{mn}^{\chi R}, \\
D_{mn}^{bs} &= \left(\frac{g_2 M_Z}{g_1 M_{Z'}} \right)^2 B_{bs}^L B_{mn}^{\chi R}, \\
\tilde{D}_{mn}^{bs} &= \left(\frac{g_2 M_Z}{g_1 M_{Z'}} \right)^2 B_{bs}^R B_{mn}^{\chi L}.
\end{aligned} \tag{2.25}$$

For convenience, in the following we will resolve the factor $g_2 M_Z / (g_1 M_{Z'})$ into the B elements or the chiral couplings.

At tree level, there are three classes of $b \rightarrow s$ transitions which are sensitive to the possible NP effects that result from an additional family non-universal $U(1)'$ symmetry: $b \rightarrow s \bar{q} q$ transitions, $b \rightarrow s \bar{l} l$ transitions, and $B_s - \bar{B}_s$ mixing. Here “q” and “l” denote quarks and leptons, respectively. For the $b \rightarrow s \bar{q} q$ transitions, the Z' effects are described by the effective Hamiltonian

$$\mathcal{H}_{\text{eff}}^{Z'}(b \rightarrow s \bar{q} q) = \frac{2G_F}{\sqrt{2}} \left((\bar{s} b)_{V-A} \sum_q (C_{qq}^{bs} (\bar{q} q)_{V-A} + D_{qq}^{bs} (\bar{q} q)_{V+A}) \right)$$

$$+(\bar{s}b)_{V+A} \sum_q \left(\tilde{D}_{qq}^{bs}(\bar{q}q)_{V-A} + \tilde{C}_{qq}^{bs}(\bar{q}q)_{V+A} \right) + \text{h.c.}, \quad (2.26)$$

in which the sum is over the active quarks for a given process. These Z' -induced FCNC effects can be understood as corrections to the SM operators or to the new penguin operators defined in Appendix A, since both lead to the same hadronic matrix elements. Explicitly, comparing Eq. (2.26) with

$$\begin{aligned} \mathcal{H}_{\text{eff}}^{Z'}(b \rightarrow s\bar{q}q) = & \\ & -\frac{G_F}{\sqrt{2}} V_{tb} V_{ts}^* \left[(\bar{s}b)_{V-A} \sum_q \left((\Delta C_3 + \Delta C_9 \frac{3}{2} e_q)(\bar{q}q)_{V-A} + (\Delta C_5 + \Delta C_7 \frac{3}{2} e_q)(\bar{q}q)_{V+A} \right) \right. \\ & \left. + (\bar{s}b)_{V+A} \sum_q \left((\Delta \tilde{C}_3 + \Delta \tilde{C}_9 \frac{3}{2} e_q)(\bar{q}q)_{V+A} + (\Delta \tilde{C}_5 + \Delta \tilde{C}_7 \frac{3}{2} e_q)(\bar{q}q)_{V-A} \right) \right] + \text{h.c.}, \end{aligned} \quad (2.27)$$

results in $4n_q$ equations (n_q is the number of active quarks in the final states):

$$\begin{aligned} \Delta C_3 + \Delta C_9 \frac{3}{2} e_q &= \frac{-2}{V_{tb} V_{ts}^*} C_{qq}^{bs}, \\ \Delta C_5 + \Delta C_7 \frac{3}{2} e_q &= \frac{-2}{V_{tb} V_{ts}^*} D_{qq}^{bs}, \\ \Delta \tilde{C}_3 + \Delta \tilde{C}_9 \frac{3}{2} e_q &= \frac{-2}{V_{tb} V_{ts}^*} \tilde{C}_{qq}^{bs}, \\ \Delta \tilde{C}_5 + \Delta \tilde{C}_7 \frac{3}{2} e_q &= \frac{-2}{V_{tb} V_{ts}^*} \tilde{D}_{qq}^{bs}, \end{aligned} \quad (2.28)$$

where ΔC denotes Z' correction to the Wilson coefficients of the SM operators and $\Delta \tilde{C}$ denotes the Wilson coefficients of the operators beyond the SM ones. For charmless processes with q from the first two families, these equations are solvable because of the following relation obeyed by the down-type quark couplings:

$$B_{11}^{\psi_{L,R}} = B_{22}^{\psi_{L,R}}, \quad (2.29)$$

which is extracted from Eq. (2.14). The Z' corrections to the Wilson coefficients are then found to be³

$$\Delta C_3 = -\frac{2}{3V_{tb} V_{ts}^*} (C_{uu}^{bs} + 2C_{dd}^{bs}), \quad \Delta C_9 = -\frac{4}{3V_{tb} V_{ts}^*} (C_{uu}^{bs} - C_{dd}^{bs}),$$

³Though the solutions to Eq. (2.28) are not unique in the case with $n_q = 1$, the physics is unaffected since it is only sensitive to the linear combinations on the left hand side of Eq. (2.28). For the charmed processes where generally we have $n_q = 1$, the formula in Eq. (2.30) can also be applied as long as Eq. (2.29) holds for the up-type quarks. If Eq. (2.29) does not hold, then the “ uu ” indices in these formula need to be replaced by “ cc ”.

$$\begin{aligned}
\Delta C_5 &= -\frac{2}{3V_{tb}V_{ts}^*} (D_{uu}^{bs} + 2D_{dd}^{bs}), & \Delta C_7 &= -\frac{4}{3V_{tb}V_{ts}^*} (D_{uu}^{bs} - D_{dd}^{bs}), \\
\Delta \tilde{C}_3 &= -\frac{2}{3V_{tb}V_{ts}^*} (\tilde{C}_{uu}^{bs} + 2\tilde{C}_{dd}^{bs}), & \Delta \tilde{C}_9 &= -\frac{4}{3V_{tb}V_{ts}^*} (\tilde{C}_{uu}^{bs} - \tilde{C}_{dd}^{bs}), \\
\Delta \tilde{C}'_5 &= -\frac{2}{3V_{tb}V_{ts}^*} (\tilde{D}_{uu}^{bs} + 2\tilde{D}_{dd}^{bs}), & \Delta \tilde{C}'_7 &= -\frac{4}{3V_{tb}V_{ts}^*} (\tilde{D}_{uu}^{bs} - \tilde{D}_{dd}^{bs}). \quad (2.30)
\end{aligned}$$

We pause here to comment on subtleties in Eq. (2.30). Recall that in the limit of small fermion mixing angles, Eq. (2.18) holds for the down-type quarks. To obtain the CKM matrix as given in Eq. (2.12) without requiring fine-tuned cancellations, the mixing angles for the up-type left-chiral quarks should also be small in this limit. Due to the $SU(2)_L$ constraint of Eq. (2.10), therefore, Eq. (2.18) can also be applied to the up-type left-chiral quarks. In this case, it is straightforward to see that

$$B_{uu}^L - B_{dd}^L \approx \tilde{\epsilon}_{uu}^L - \tilde{\epsilon}_{dd}^L \equiv 0, \quad (2.31)$$

and hence

$$\begin{aligned}
\Delta C_9 &\approx 0, & \Delta \tilde{C}_7 &\approx 0, \\
\Delta C_3 &\approx -\frac{2}{V_{tb}V_{ts}^*} C_{dd}^{bs}, & \Delta \tilde{C}_5 &\approx -\frac{2}{V_{tb}V_{ts}^*} \tilde{D}_{dd}^{bs}. \quad (2.32)
\end{aligned}$$

Note that a relation similar to Eq.(2.10) does not exist for the right-chiral SM fermions, so ΔC_7 and $\Delta \tilde{C}_9$ are generically non-trivial. In regards to the color-allowed penguin operators, their Wilson coefficients are corrected by Z' effects only at the loop level where the color-indices are mixed by gluons. Since these effects suffer loop and Z' mass double suppressions, we will not consider them further in this paper.

For the $b \rightarrow s\bar{l}l$ transitions, the Z' contributions to the effective Hamiltonian are

$$\begin{aligned}
\mathcal{H}_{\text{eff}}^{Z'}(b \rightarrow s\bar{l}l) &= \frac{2G_F}{\sqrt{2}} \left((\bar{s}b)_{V-A} (C_{ll}^{bs} (\bar{l}l)_{V-A} + D_{ll}^{bs} (\bar{l}l)_{V+A}) \right. \\
&\quad \left. + (\bar{s}b)_{V+A} (\tilde{D}_{ll}^{bs} (\bar{l}l)_{V-A} + \tilde{C}_{ll}^{bs} (\bar{l}l)_{V+A}) \right) + \text{h.c.} \quad (2.33)
\end{aligned}$$

Comparing Eq. (2.33) with

$$\begin{aligned}
\mathcal{H}_{\text{eff}}^{Z'}(b \rightarrow s\bar{l}l) &= -\frac{G_F}{\sqrt{2}} V_{tb}V_{ts}^* \left(\Delta C_{9V} Q_{9V} + \Delta C_{10A} Q_{10A} \right. \\
&\quad \left. + \Delta \tilde{C}_{9V} \tilde{Q}_{9V} + \Delta \tilde{C}_{10A} \tilde{Q}_{10A} \right) + \text{h.c.}, \quad (2.34)
\end{aligned}$$

one can see that the Z' corrections to the Wilson coefficients take the following form:

$$\begin{aligned}
\Delta C_{9V} &= -\frac{2}{V_{tb}V_{ts}^*} (C_{ll}^{bs} + D_{ll}^{bs}), \\
\Delta C_{10A} &= -\frac{2}{V_{tb}V_{ts}^*} (-C_{ll}^{bs} + D_{ll}^{bs}),
\end{aligned}$$

$$\begin{aligned}
\Delta\tilde{C}_{9V} &= -\frac{2}{V_{tb}V_{ts}^*}(\tilde{C}_{ll}^{bs} + \tilde{D}_{ll}^{bs}), \\
\Delta\tilde{C}_{10A} &= -\frac{2}{V_{tb}V_{ts}^*}(\tilde{C}_{ll}^{bs} - \tilde{D}_{ll}^{bs}).
\end{aligned} \tag{2.35}$$

Note that if the leptons in the process are neutrinos, Eqs. (2.35) reduces to

$$\begin{aligned}
\Delta C_{9V} &= -\frac{2}{V_{tb}V_{ts}^*}C_{ll}^{bs}, \\
\Delta C_{10A} &= \frac{2}{V_{tb}V_{ts}^*}C_{ll}^{bs}, \\
\Delta\tilde{C}_{9V} &= -\frac{2}{V_{tb}V_{ts}^*}\tilde{D}_{ll}^{bs}, \\
\Delta\tilde{C}_{10A} &= \frac{2}{V_{tb}V_{ts}^*}\tilde{D}_{ll}^{bs},
\end{aligned} \tag{2.36}$$

since right-handed neutrinos are generally decoupled at low energy scales.

For $B_s - \bar{B}_s$ mixing, the Z' corrections to the effective Hamiltonian take the form

$$\begin{aligned}
\mathcal{H}_{\text{eff}}^{Z'}(B_s - \bar{B}_s) &= \frac{G_F}{\sqrt{2}} \left(C_{bs}^{bs}(\bar{s}b)_{V-A}(\bar{s}b)_{V-A} + D_{bs}^{bs}(\bar{s}b)_{V-A}(\bar{s}b)_{V+A} \right. \\
&\quad \left. + \tilde{D}_{bs}^{bs}(\bar{s}b)_{V+A}(\bar{s}b)_{V-A} + \tilde{C}_{bs}^{bs}(\bar{s}b)_{V+A}(\bar{s}b)_{V+A} \right) + \text{h.c.}
\end{aligned} \tag{2.37}$$

Once again, upon comparing this expression to

$$\mathcal{H}_{\text{eff}}^{Z'}(B_s - \bar{B}_s) = -\frac{G_F}{\sqrt{2}} \left(\Delta C_1^{B_s} Q_1^{B_s} + \Delta\tilde{C}_1^{B_s} \tilde{Q}_1^{B_s} + 2\Delta\tilde{C}_3^{B_s} \tilde{Q}_3^{B_s} \right) + \text{h.c.}, \tag{2.38}$$

the Z' corrections to the Wilson coefficients are easily determined to be

$$\begin{aligned}
\Delta C_1^{B_s} &= -C_{bs}^{bs}, \\
\Delta\tilde{C}_1^{B_s} &= -\tilde{C}_{bs}^{bs} \\
\Delta\tilde{C}_3^{B_s} &= -\frac{1}{2}(D_{bs}^{bs} + \tilde{D}_{bs}^{bs}) = -\tilde{D}_{bs}^{bs}.
\end{aligned} \tag{2.39}$$

As in the $b \rightarrow s\bar{q}q$ transitions, the Z' effects only correct the Wilson coefficients of the color-allowed operators at a higher loop level, so we will not consider them further here.

To summarize, in Table (3) we classify the tree-level Z' contributions to the $b \rightarrow s$ transitions according to whether they are relevant or irrelevant to the SM operators.

Before considering the general parameter space, it is worthwhile to consider a few special limits: (1) the LR limit: $|B_{bs}^L| = |B_{bs}^R|$, $\phi_{bs}^L = \phi_{bs}^R$; (2) the LL limit: $\epsilon^{\psi_R} \propto I$; and (3) the RR limit: $\epsilon^{\psi_L} \propto I$, where I is the identity. The Z' corrections to the Wilson coefficients in these limits are summarized as follows:

Table 3: Classification of the tree-level Z' corrections to the Wilson coefficients in the $b \rightarrow s$ transitions.

	SM operators	Beyond SM Operators
$b \rightarrow s\bar{q}q$	$\Delta C_a, a = 3, 5, 7$	$\Delta\tilde{C}_a, a = 3, 5, 9$
$b \rightarrow s\bar{l}l$	$\Delta C_a, a = 9V, 10A$	$\Delta\tilde{C}_a, a = 9V, 10A$
$B_s - \bar{B}_s$ mixing	$\Delta C_1^{B_s}$	$\Delta\tilde{C}_a^{B_s}, a = 1, 3$

(1) **LR limit:** $B_{bs}^L = B_{bs}^R$.

$$\begin{aligned}
\Delta C_1^{B_s} &= \Delta\tilde{C}_1^{B_s} = \Delta\tilde{C}_3^{B_s} = -(B_{bs}^L)^2, \\
\Delta C_3 &= \Delta\tilde{C}_5 = -\frac{2}{V_{tb}V_{ts}^*}B_{bs}^L B_{dd}^L, \\
\Delta\tilde{C}_3 &= \Delta C_5 = -\frac{2}{3V_{tb}V_{ts}^*}B_{bs}^L (B_{uu}^R + 2B_{dd}^R), \\
\Delta C_7 &= \Delta\tilde{C}_9 = -\frac{4}{3V_{tb}V_{ts}^*}B_{bs}^L (B_{uu}^R - B_{dd}^R), \\
\Delta C_{9V} &= \Delta\tilde{C}_{9V} = -\frac{2}{V_{tb}V_{ts}^*}B_{bs}^L (B_{ll}^L + B_{ll}^R), \\
\Delta C_{10A} &= \Delta\tilde{C}_{10A} = -\frac{2}{V_{tb}V_{ts}^*}B_{bs}^L (-B_{ll}^L + B_{ll}^R).
\end{aligned} \tag{2.40}$$

(2) **LL limit:** $\epsilon^{\psi_R} \propto I$.

$$\begin{aligned}
\Delta C_1^{B_s} &= -(B_{bs}^L)^2, \\
\Delta C_3 &= -\frac{2}{V_{tb}V_{ts}^*}B_{bs}^L B_{dd}^L, \\
\Delta C_5 &= -\frac{2}{3V_{tb}V_{ts}^*}B_{bs}^L (B_{uu}^R + 2B_{dd}^R), \\
\Delta C_7 &= -\frac{4}{3V_{tb}V_{ts}^*}B_{bs}^L (B_{uu}^R - B_{dd}^R), \\
\Delta C_{9V} &= -\frac{2}{V_{tb}V_{ts}^*}B_{bs}^L (B_{ll}^L + B_{ll}^R), \\
\Delta C_{10A} &= -\frac{2}{V_{tb}V_{ts}^*}B_{bs}^L (-B_{ll}^L + B_{ll}^R).
\end{aligned} \tag{2.41}$$

(3) **RR limit:** $\epsilon^{\psi_L} \propto I$.

$$\Delta\tilde{C}_1^{B_s} = -(B_{bs}^R)^2,$$

$$\begin{aligned}
\Delta\tilde{C}_3 &= -\frac{2}{3V_{tb}V_{ts}^*}B_{bs}^R(B_{uu}^R + 2B_{dd}^R), \\
\Delta\tilde{C}_5 &= -\frac{2}{V_{tb}V_{ts}^*}B_{bs}^RB_{dd}^L, \\
\Delta\tilde{C}_9 &= -\frac{4}{3V_{tb}V_{ts}^*}B_{bs}^R(B_{uu}^R - B_{dd}^R), \\
\Delta\tilde{C}_{9V} &= -\frac{2}{V_{tb}V_{ts}^*}B_{bs}^R(B_{ll}^L + B_{ll}^R), \\
\Delta\tilde{C}_{10A} &= -\frac{2}{V_{tb}V_{ts}^*}B_{bs}^R(-B_{ll}^L + B_{ll}^R).
\end{aligned} \tag{2.42}$$

We will focus on the correlations between $B_s - \bar{B}_s$ mixing and the hadronic B_d meson decays. For the latter, though Z' -mediated effects can occur in both the QCD and EW penguins, we make a conservative assumption in this paper that they are mainly manifest in the EW penguins, such that $|\Delta C_{3,5}| \ll |\Delta C_7|$, as suggested in [17, 15]. With this restriction, there are only three relevant parameters for each special limit: the modulus of B_{bs}^L (or B_{bs}^R), its phase ϕ_{bs}^L (or ϕ_{bs}^R), and the real B_{dd}^R ($\simeq -B_{uu}^R/2$). These parameters need to satisfy

$$|B_{bs}^L| < |B_{dd}^L| \ll |B_{dd}^R| \tag{2.43}$$

in the LR and LL limits, and

$$|B_{bs}^R| < |B_{dd}^R|, \quad |B_{dd}^L| \ll |B_{dd}^R| \tag{2.44}$$

in the RR limit. Here $|B_{bs}^{L,R}| < |B_{dd}^{L,R}|$ is due to the fact that, under the assumption of small fermion mixing angles, the modulus of off-diagonal elements in the coupling matrix in Eq. (2.14) should be smaller than that of diagonal ones; $|B_{dd}^L| \ll |B_{dd}^R|$ is due to $|\Delta C_{3,5}| \ll |\Delta C_7|$. Later in the paper, we will consider the more general parameter space for the Z' -mediated effects in the EW penguins, which has five free parameters: $|B_{bs}^{L,R}|$, $\phi_{bs}^{L,R}$ and B_{dd}^R .

2.2 Effective Couplings at the b Mass Scale

To achieve sufficient precision for these observables, it is necessary to have an accurate knowledge of the relevant Wilson coefficients at the b quark mass scale $m_b = 4.2$ GeV. The Wilson coefficients at the b mass scale can be obtained as follows:

$$\vec{C}(m_b) = U(m_b, M_W) \vec{C}(M_W), \tag{2.45}$$

where \vec{C} is a vector with entries consisting of the Wilson coefficients and U is the evolution matrix. The observables can then be expressed in terms of the Wilson coefficients at the m_b scale (for general discussions, see e.g. [18]). All parameter values used in our calculations are summarized in Appendix C.

• **B_s mixing.** Following [18], the NP probes C_{B_s} and ϕ_{B_s} , which are defined in Eq. (1.1), are calculated to be

$$C_{B_s} e^{2i\phi_{B_s}} = 1 - 3.59 \times 10^5 (\Delta C_1^{B_s} + \Delta \tilde{C}_1^{B_s}) + 2.04 \times 10^6 \Delta \tilde{C}_3^{B_s} \quad (2.46)$$

at the m_b scale. The large coefficients of the correction terms are due to the fact that the NP is introduced at tree-level while the SM limit is a loop-level effect.

• **$B_d \rightarrow \pi K_S$ decays.** The $B_d \rightarrow \pi K_S$ decays have recently received considerable interest in the literature (see e.g. [17, 19, 20, 21, 22, 23]). In [17], it is pointed out that a deviation of $\mathcal{S}_{\pi K_S}$ from its SM value can be understood as a modification of the ratio

$$qe^{i\phi} = \frac{P}{T + C}, \quad (2.47)$$

in which T , C and P denote the color-allowed tree, color-suppressed tree, and EW penguin contributions in the decay amplitude, respectively. In the class of models considered here, the family non-universal Z' interactions modify $qe^{i\phi}$ through the relation

$$qe^{i\phi} = 0.76(1 + 158.1\Delta C_7 - 102.4\Delta \tilde{C}_9), \quad (2.48)$$

in which q and ϕ are given by 0.76 and zero, respectively, in the SM limit.

• **$B_d \rightarrow (\psi, \phi, \eta', \rho, \omega, f^0) K_S$ decays.** The direct and the mixing-induced CP asymmetries in the B_d hadronic decays are parametrized as follows:

$$\mathcal{C}_{f_{CP}} = \frac{1 - |\lambda_{f_{CP}}|^2}{1 + |\lambda_{f_{CP}}|^2}, \quad \mathcal{S}_{f_{CP}} = \frac{2\text{Im}[\lambda_{f_{CP}}]}{1 + |\lambda_{f_{CP}}|^2}. \quad (2.49)$$

In the above, $\lambda_{f_{CP}}$ is defined by

$$\lambda_{f_{CP}} \equiv -\eta_{f_{CP}} \frac{q_{B_d} \bar{A}_{f_{CP}}}{p_{B_d} A_{f_{CP}}}, \quad (2.50)$$

with

$$\frac{q_{B_d}}{p_{B_d}} \Big|_{\Delta\Gamma_{B_d}=0} = -\frac{(M_{B_d})_{12}^*}{|(M_{B_d})_{12}|} = -e^{-2i\phi_{B_d}}. \quad (2.51)$$

Here q_{B_d} and p_{B_d} are B_d mixing coefficients

$$\begin{aligned} |B_L\rangle &= p_{B_d}|B_d\rangle + q_{B_d}|\bar{B}_d\rangle \\ |B_H\rangle &= p_{B_d}|B_d\rangle - q_{B_d}|\bar{B}_d\rangle, \end{aligned} \quad (2.52)$$

M_{B_d} is the $B_d - \bar{B}_d$ mass matrix, and $A_{f_{CP}}$ is the decay amplitude of $B_d \rightarrow f_{CP}$ ($\bar{A}_{f_{CP}}$ is its CP conjugate.).

The SM predicts that $\phi_{B_d} = \beta \equiv \arg[-(V_{cd}V_{cb}^*)/(V_{td}V_{tb}^*)]$ and that a non-trivial weak phase enters $A_{f_{CP}}$ only at order $\mathcal{O}(\lambda^2)$. Therefore, for time-dependent decays proceeding via $b \rightarrow s\bar{q}q$ ($q = u, d, c, s$), including $B_d \rightarrow \psi K_S$ and penguin-dominated modes such as $B_d \rightarrow (\phi, \eta', \pi, \rho, \omega, f^0)K_S$, the relations in Eq. (1.4) are obtained. However, these results are greatly changed with the involvement of family non-universal Z' bosons, since this allows for a new weak phase to enter $A_{f_{CP}}$ at tree level. Following Ali et. al. [24], the $\lambda_{f_{CP}}$ parameters of $B_d \rightarrow (\psi, \phi, \eta', \pi, \rho, \omega, f^0)K_S$ are given by

$$\lambda_{\psi K_S} = \frac{(-0.63 + 0.74i)}{1 + (0.18 - 0.01i)(\Delta C_7 + \Delta \tilde{C}_7)^* - (0.06 - 0.04i)(\Delta C_9 + \Delta \tilde{C}_9)^*} \frac{(2.53)}{1 + (0.17 + 0.01i)(\Delta C_7 + \Delta \tilde{C}_7) - (0.05 + 0.05i)(\Delta C_9 + \Delta \tilde{C}_9)},$$

$$\lambda_{\phi K_S} = \frac{(-0.70 + 0.70i)}{1 + (14.57 + 5.88i)(\Delta C_7 + \Delta \tilde{C}_7)^* + (15.08 + 5.92i)(\Delta C_9 + \Delta \tilde{C}_9)^*} \frac{(2.54)}{1 + (14.39 + 5.64i)(\Delta C_7 + \Delta \tilde{C}_7) + (14.90 + 5.66i)(\Delta C_9 + \Delta \tilde{C}_9)},$$

$$\lambda_{\eta' K_S} = \frac{(-0.70 + 0.69i)}{1 + (2.11 + 0.67i)(\Delta C_7 + \Delta \tilde{C}_7)^* + (2.10 + 0.54i)(\Delta C_9 + \Delta \tilde{C}_9)^*} \frac{(2.55)}{1 + (2.08 + 0.65i)(\Delta C_7 + \Delta \tilde{C}_7) + (2.07 + 0.52i)(\Delta C_9 + \Delta \tilde{C}_9)},$$

$$\lambda_{\rho K_S} = \frac{(-0.74 + 0.66i)}{1 - (38.75 + 3.29i)(\Delta C_7 + \Delta \tilde{C}_7)^* - (47.95 + 4.11i)(\Delta C_9 + \Delta \tilde{C}_9)^*} \frac{(2.56)}{1 - (38.11 + 5.23i)(\Delta C_7 + \Delta \tilde{C}_7) - (47.15 + 6.50i)(\Delta C_9 + \Delta \tilde{C}_9)},$$

$$\lambda_{\omega K_S} = \frac{(-0.71 + 0.70i)}{1 + (31.97 + 4.76i)(\Delta C_7 + \Delta \tilde{C}_7)^* + (18.84 + 2.75i)(\Delta C_9 + \Delta \tilde{C}_9)^*} \frac{(2.57)}{1 + (31.81 + 4.67i)(\Delta C_7 + \Delta \tilde{C}_7) + (18.74 + 2.70i)(\Delta C_9 + \Delta \tilde{C}_9)},$$

$$\lambda_{f^0 K_S} = \frac{(-0.70 + 0.70i)}{1 + (3.19 + 0.93i)(\Delta C_7 + \Delta \tilde{C}_7)^* - (0.12 + 0.15i)(\Delta C_9 + \Delta \tilde{C}_9)^*} \frac{(2.58)}{1 + (3.16 + 0.90i)(\Delta C_7 + \Delta \tilde{C}_7) - (0.12 + 0.15i)(\Delta C_9 + \Delta \tilde{C}_9)}.$$

In contrast to the $B_d \rightarrow \psi K_S$ decay, in which the NP effects are suppressed by the SM tree-level contribution, family non-universal $U(1)'$ couplings indeed result in sizable corrections to $\lambda_{f_{CP}}$ for the penguin-dominated modes.

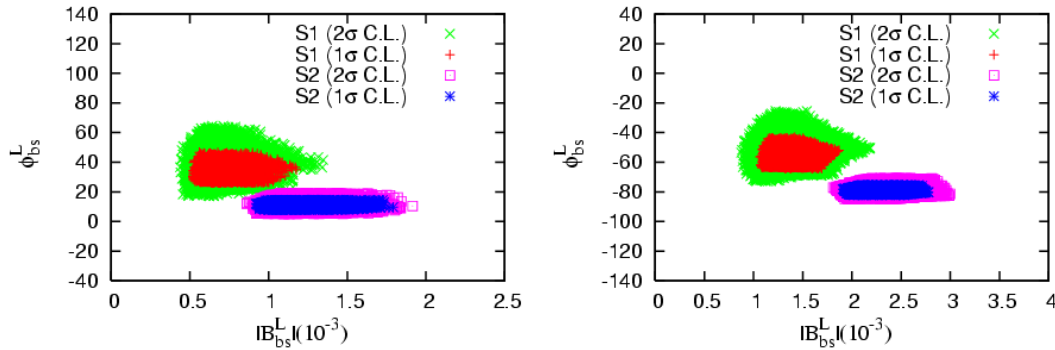


Figure 1: Correlated constraints on $|B_{bs}^L|$ and ϕ_{bs}^L are presented. In these two panels, random values for C_{B_s} and $\phi_{B_s}^{\text{NP}}$ from the experimentally allowed regions (see Table 1) are mapped to the $|B_{bs}^L| - \phi_{bs}^L$ plane using Eq. (3.59), with an assumed 25% uncertainty (a typical value from non-perturbative effects) assumed for the coefficients. The left (right) panel is the LR (LL) limit.

3 Results and Analysis

3.1 Correlated Analysis (I) – Special Limits

In this section, we will present a correlated analysis of the $\Delta B = 1, 2$ processes which occur via $b \rightarrow s$ transitions, focusing first on the special limits of the parameter space as presented in Section 2.1. As the physics of the RR limit is very similar to that of the LL limit, we focus in this paper on the LR and LL limits as representative examples.

We first consider the constraints on this class of family non-universal $U(1)'$ scenarios which arise from $B_s - \bar{B}_s$ mixing. With the renormalization scale chosen as the b -quark mass, $m_b = 4.2$ GeV, the NP probes C_{B_s} and $\phi_{B_s}^{\text{NP}}$ are given by

$$\begin{aligned} C_{B_s} e^{2i\phi_{B_s}^{\text{NP}}} &= 1 + 1.32 \times 10^6 \Delta C_1^{B_s} \\ C_{B_s} e^{2i\phi_{B_s}^{\text{NP}}} &= 1 - 3.59 \times 10^5 \Delta \tilde{C}_1^{B_s} \end{aligned} \quad (3.59)$$

in the LR and LL limits, respectively. These conditions involve two of the three free parameters of each limit: $|B_{bs}^L|$ and ϕ_{bs}^L . The experimental constraints on these parameters from $B_s - \bar{B}_s$ mixing are illustrated in Fig. 1. The left panel corresponds to the LR limit and the right one corresponds to the LL limit; in this section we will present the results for these two limits together, so that it is easy to make comparisons between the two cases. In each case, there are two separate shaded regions, corresponding to the two $\phi_{B_s}^{\text{NP}}$ solutions (see Table 1). For each region, the various colors of the points specify the different confidence levels (C.L.) of the relevant C_{B_s} and $\phi_{B_s}^{\text{NP}}$ values. To explain the observed discrepancy in $B_s - \bar{B}_s$ mixing from the SM prediction, $|B_{bs}^L|$ is required to be $\sim 10^{-3}$. This reflects two facts: (1) unlike $\phi_{B_s}^{\text{NP}}$, the modulus C_{B_s} does not deviate from its SM prediction significantly (the experimental value of C_{B_s} has an at most $\mathcal{O}(1)$ shift

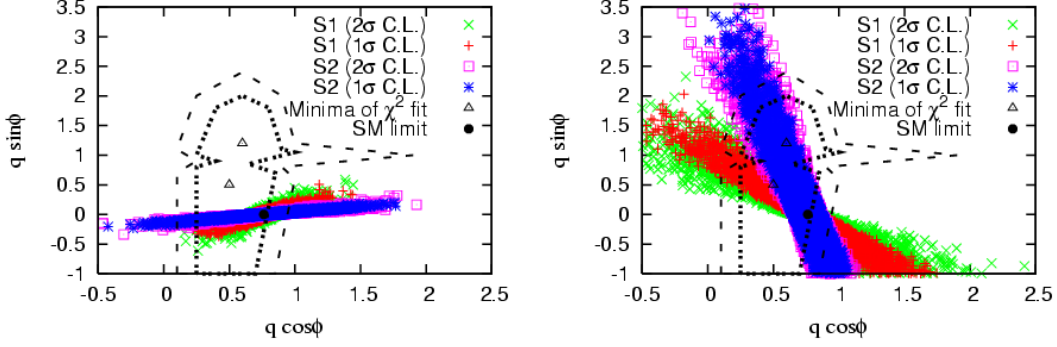


Figure 2: The constraints on B_{dd}^R from $qe^{i\phi}$ are shown. The points from the $|B_{bs}^L| - \phi_{bs}^L$ plane (see Fig. 1) are randomly combined with scattered points of B_{dd}^R ($10^{-3} \leq |B_{dd}^R| \leq 10^{-1}$) and then mapped to the $q \cos \phi - q \sin \phi$ plane according to Eq. (3.64). The colors of the points in this plane indicate the C.L. that their inverse images represent in Fig. 1. The two dashed lines specify the experimentally allowed ranges that result from the χ^2 fit of the $B \rightarrow \pi K$ (and $B \rightarrow \pi\pi$) data at 1σ and 90% ($\simeq 1.7\sigma$) C.L., respectively [19]. The left (right) panels are the LR (LL) limits.

from its SM prediction at 2σ C.L.); (2) the Z' corrections are from tree level, and hence can easily explain this small deviation (only a small coupling is necessary, according to Eq. (3.59) and Eq. (2.40), Eq. (2.41)). The smallness of $|B_{bs}^L|$ is generically consistent with our assumption of small fermion mixing angles, since B_{bs}^L is proportional to them as well as to $g_2 M_Z / (g_1 M_{Z'})$ (see Eq. (2.18) and the comments under Eq. (2.25)). In addition, due to the smallness of $|B_{bs}^L|$, the experimental constraints from the branching ratio $\text{Br}(B_s \rightarrow \mu^+ \mu^-)$ can be easily satisfied. For details, see Appendix B.

Before move to the other $b \rightarrow s$ processes, we have some comments on the influence of $B_s - \bar{B}_s$ mixing on another FCNC Z' coupling $B_{bd}^{L,R}$. In the SM, the mass differences of B_d and B_s mesons are predicted to be (e.g., see [25])

$$\begin{aligned} \Delta M_d^{\text{SM}} &= (0.53 \pm 0.02) \left(\frac{|V_{td}|}{0.0082} \right)^2 \left(\frac{f_{B_d}}{200 \text{MeV}} \right)^2 \frac{B}{0.85} \text{ps}^{-1} \\ \Delta M_s^{\text{SM}} &= (19.3 \pm 0.6) \left(\frac{|V_{ts}|}{0.00405} \right)^2 \left(\frac{f_{B_s}}{240 \text{MeV}} \right)^2 \frac{B}{0.85} \text{ps}^{-1} \end{aligned} \quad (3.60)$$

with f_{B_d, B_s} being decay constant of $B_d(B_s)$ and B being bag factor. Comparing with the experimental data [26]

$$\begin{aligned} \Delta M_d &= \Delta M_d^{\text{SM}} \left(1 + \frac{\Delta M_d^{\text{NP}}}{\Delta M_d^{\text{SM}}} \right) = 0.507 \pm 0.005 \text{ps}^{-1} \\ \Delta M_s &= \Delta M_s^{\text{SM}} \left(1 + \frac{\Delta M_s^{\text{NP}}}{\Delta M_s^{\text{SM}}} \right) = 17.77 \pm 0.12 \text{ps}^{-1}, \end{aligned} \quad (3.61)$$

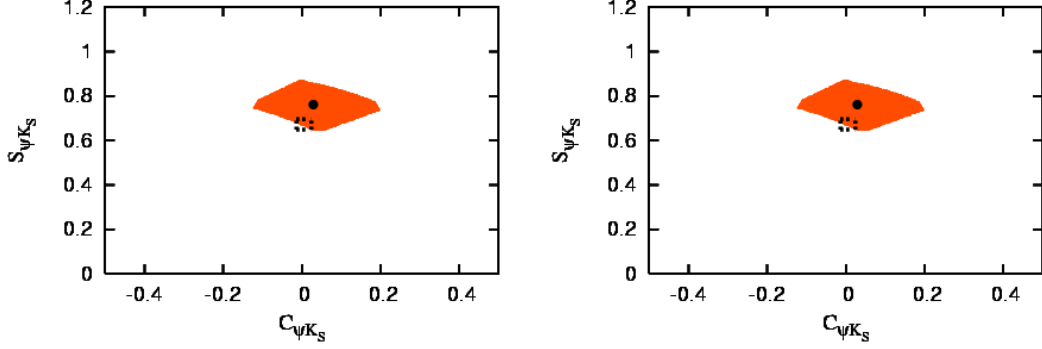


Figure 3: The time-dependent CP asymmetries of the charmed $B_d \rightarrow \psi K_S$ decay are presented (with $|V_{ub}| = 3.51 \times 10^{-3}$, as is used in the SM calculation [28]). The box is at 1σ C.L. and the dark point is the SM limit. The left (right) panels are the LR (LL) limits.

we have the relation

$$\frac{\Delta M_d^{\text{NP}}}{\Delta M_d^{\text{SM}}} \sim \frac{\Delta M_s^{\text{NP}}}{\Delta M_s^{\text{SM}}} \quad (3.62)$$

with

$$\frac{\Delta M_d^{\text{NP}}}{\Delta M_s^{\text{NP}}} \sim \frac{|B_{bd}^{L,R}|^2}{|B_{bs}^{L,R}|^2}, \quad \frac{\Delta M_d^{\text{SM}}}{\Delta M_s^{\text{SM}}} \sim \lambda^2 \approx 0.04. \quad (3.63)$$

But, according to Eq. (2.18), the modulus of $B_{bd}^{L,R}$ usually is comparable with that of $B_{bs}^{L,R}$, a fine-tuning of $\mathcal{O}(10\%)$ level therefore is needed in $|B_{bd}^{L,R}|$ to satisfy the experimental constraints from ΔM_d . In this paper, we will work under the assumption of negligible $|B_{bd}^{L,R}|$, and therefore will neglect its possible effect in the NP observables.

The second process of interest is $B_d \rightarrow \pi K_S$. The time-dependent CP asymmetries of these decays can be sizably affected by NP, as has been pointed out in [17]. The experimental constraints on $qe^{i\phi}$ (defined in Eq. (2.47)) for different C.L.'s from the $B \rightarrow \pi K$ (and the $B \rightarrow \pi\pi$) data have previously been obtained in [19]. In Fig. 2, we illustrate how B_{dd}^R is constrained through $qe^{i\phi}$, using the parameter values of $|B_{bs}^L|$ and ϕ_{bs}^L obtained in Fig. 1, along with the following relations:

$$\begin{aligned} qe^{i\phi} &= 0.76(1 + 55.7\Delta C_7) \\ qe^{i\phi} &= 0.76(1 + 158.1\Delta C_7), \end{aligned} \quad (3.64)$$

which are valid in the LR and LL limits, respectively. There are two distribution regions which are specified by different colors in each panel, again due to the two $\phi_{B_s}^{\text{NP}}$ solutions. Note that in the LL limit, the shaded region passes through both of the minimal points that were found in the χ^2 fit of the $B \rightarrow \pi K$ and $B \rightarrow \pi\pi$ data in [19].

In the scenarios under consideration, the constraints from $B_s - \bar{B}_s$ mixing and $B_d \rightarrow \pi K_S$ decays place bounds on each of the three free parameters $|B_{bs}^L|$, ϕ_{bs}^L and B_{dd}^R . The natural question is then whether the experimentally allowed values for these parameters also satisfy the constraints resulting from the possibly anomalous values of $\Delta\mathcal{C}_{f_{CP}}$ and $\Delta\mathcal{S}_{f_{CP}}$ in the remaining penguin-dominated $B_d \rightarrow (\phi, \eta', \rho, \omega, f_0)K_S$ decays. To address this issue, we assume a 15% uncertainty in the SM calculations for each of these modes (as well as for the $B_d \rightarrow \pi K_S$ mode) and a 25% uncertainty for the NP contributions. Here 15% is a typical uncertainty level for the hadronic matrix elements of the SM FC operators (e.g., see [27]) and is also the least necessary one to explain the experimental data of $\mathcal{C}_{\psi K_S}$ and $\mathcal{S}_{\psi K_S}$ in the SM (see Fig. 3 where the NP effects are negligible). As for the difference of the uncertainty levels between the SM and NP calculations, it is caused by the fact that the hadronic matrix elements of the FC operators in the SM are better understood than they are for the NP operators. In Fig. 4, we systematically illustrate the time-dependent CP asymmetries in the penguin-dominated modes, using the parameter values obtained above and Eqs. (2.53)–(2.58). For these modes with the exception of $B_d \rightarrow \rho K_S$, there are $0.5 \sim 2\sigma$ deviations for $\mathcal{C}_{f_{CP}}$, $\mathcal{S}_{f_{CP}}$, or both. Though our model only induces negligible effects on $B_d - \bar{B}_d$ mixing under the assumption of small $|B_{bd}|$, due to the interference effects between the $B_d - \bar{B}_d$ mixing phase and ϕ_{bs}^L which affects the decay asymmetries $\frac{\bar{A}_{f_{CP}}}{A_{f_{CP}}}$ in Eq. (2.50), the points in Fig. 4 are scattered away from the SM limits. This results in a dispersion such that there are always some points lying in the 1σ region for each of these modes.

To show that all of the constraints can be satisfied simultaneously, we have carried out a correlated analysis among the $B_s - \bar{B}_s$ mixing and the $B_d \rightarrow (\pi, \phi, \eta', \rho, \omega, f_0)K_S$ CP asymmetries. The allowed values for $|B_{bs}^L|$, ϕ_{bs}^L and B_{dd}^R in the LR and LL limits are illustrated in Fig. 5. We see that in Fig. 5 there indeed exist parameter regions where the anomalies in $B_s - \bar{B}_s$ mixing and the time-dependent CP asymmetries of $B_d \rightarrow (\pi, \phi, \eta', \rho, \omega, f_0)K_S$, can be explained by NP at reasonable C.L.. The allowed $|B_{bs}^R|$ and ϕ_{bs}^L values can explain both solutions of $B_s - \bar{B}_s$ mixing phase; and the allowed $|B_{dd}^R|$ values vary from 0.08 to smaller values. If we want to get a better fit for $\mathcal{C}_{(\pi, \phi, \eta', \rho, \omega, f_0)K_S}$ and $\mathcal{S}_{(\pi, \phi, \eta', \rho, \omega, f_0)K_S}$, $|B_{dd}^R| \gtrsim 10^{-2}$ is typically required. To see this point, we take for example $\mathcal{C}_{\pi K_S}$ and $\mathcal{S}_{\pi K_S}$, and map the points in Fig. 5 back to the $q \cos \phi - q \sin \phi$ plane, as illustrated in Fig 6. In this figure we see that the points with $B_{dd}^R < -0.01$ are closer to the minima of the χ^2 fit of the $B \rightarrow \pi K$ and $B \rightarrow \pi\pi$ data, leading to a better fit compared to the one obtained in the SM limit. Therefore, $|B_{dd}^R| \gtrsim 10^{-2}$ is important in improving the agreement with experimental data in the penguin-dominated B_d decays.⁴

The favored parameter values for $|B_{dd}^R|$ are interesting for collider detection. For $(V_{dR} \tilde{e}^{dR} V_{dR})_{11} \sim \mathcal{O}(1)$, this implies that $g_1 M_{Z'}/(g_2 M_Z) \sim 10 - 100$ or a TeV scale Z' boson for $g_2 \lesssim g_1$, a range approachable at the LHC (e.g., see [12, 29]). This fact is also important for the effective Lagrangian in Eq. (2.20) which is obtained by integrating out the Z' boson. While applying it to our analysis, we neglected the effects of the

⁴This effect can also be seen by requiring a smaller C.L. for the fit of $\mathcal{C}_{(\phi, \eta', \rho, \omega, f_0)K_S}$ and $\mathcal{S}_{(\phi, \eta', \rho, \omega, f_0)K_S}$, which has been shown in the LR limit in Fig. 4 of [14].

renormalization group running between Z' mass scale and EW scale, which is justified only for a small gap between these two scale or for a low-scale Z' boson. In addition, we emphasize that the favored parameter regions are consistent with our assumption that the non-universal Z' effects in QCD penguins are negligible. This assumption requires $|\Delta C_{3,5}| \ll |\Delta C_7|$ or $|B_{bs}^L| < |B_{dd}^L| \ll |B_{dd}^R|$. Since $|B_{bs}^L|$ and $|B_{dd}^R|$ are favored to be $\sim 10^{-3}$ and $\gtrsim 10^{-2}$ respectively, this relation can be easily accommodated. At last, to implement our discussions, we take a χ^2 fit in the SM and in the non-universal $U(1)'$ models for all relevant observables except $qe^{i\phi}$. We find that the reduced χ^2 value (*i.e.*, $\chi^2/\text{D.O.F.}$) in the SM is larger than 2, and that of the best fit in both LL and LR limits in the $U(1)'$ models is smaller than 1. Therefore, a better fit is obtained in the latter.

3.2 Correlated Analysis (II) – General Case

As discussed in Section 2.1, there are five free parameters in the general case: $|B_{bs}^{L,R}|$, $\phi_{bs}^{L,R}$, and B_{dd}^R . Let us focus first on $B_s - \bar{B}_s$ mixing again. The general relation in Eq. (2.46) involves four of the five free parameters: $|B_{bs}^{L,R}|$ and $\phi_{bs}^{L,R}$. In Fig. 7, we show how the experimentally allowed parameter values are distributed. For each of the two top panels in Fig. 7, there are two peaks and two valleys toward the right. The two peaks in the left panel correspond to the LL limit, and the two in the right panel correspond to the RR limit. Meanwhile, the points in the right panel which are associated with the LL limit and the points in the left panel which are associated with the RR limit are localized in the regions $|B_{bs}^L| \approx 0$ and $|B_{bs}^R| \approx 0$, respectively. As for the valleys in both panels, they correspond to the LR limit. Observe that there are two solutions for each of these three limits which are specified by a difference of 180° either in ϕ_{bs}^L or ϕ_{bs}^R (or both). We only showed one of the two solutions in Fig. 1, since the difference between these two solutions can be resolved into B_{dd}^R as a minus sign. For the two bottom panels, the three special limits LL, LR and RR correspond to the bottom boundary, the diagonal line (the one from left-bottom to right-up) and the left boundary in the left one, respectively. Clearly, for the LL (RR) limit, $|B_{bs}^L|$ ($|B_{bs}^R|$) has a relatively large value compared to the one in the LR limit, as seen in Fig. 1. In the right panel, these three limits correspond to the two parallel bands $\phi_{bs}^L \sim -50^\circ, 130^\circ$, the diagonal line (the one from left-bottom to right-up) and the two parallel bands $\phi_{bs}^R \sim -50^\circ, 130^\circ$, respectively.

In Fig. 8, we illustrate how the yet free parameter B_{dd}^R is constrained through $qe^{i\phi}$, using the parameter values of $|B_{bs}^{L,R}|$ and $\phi_{bs}^{L,R}$ obtained in Fig. 7, the relation Eq. (2.48), and the allowed range for $qe^{i\phi}$ as determined in [19]. Compare this figure with Fig. 2 we see that our scan selects points which are more likely to be associated with the solution “S1” of $B_s - \bar{B}_s$ mixing. To see the reason, let us rewrite Eq. (2.46) as

$$\begin{aligned} \frac{A_s^{\text{NP}}}{A_s^{\text{SM}}} e^{2i\phi_s^{\text{NP}}} &= 3.59 \times 10^5 (|B_{bs}^L|^2 e^{2i\phi_{bs}^L} + |B_{bs}^R|^2 e^{2i\phi_{bs}^R}) \\ &\quad - 2.04 \times 10^6 |B_{bs}^L B_{bs}^R| e^{i(\phi_{bs}^L + \phi_{bs}^R)} \end{aligned} \quad (3.65)$$

by using the relation Eq. (1.2). Since the range of the solution “S1” is much larger than that of the solution “S2” at the same C.L. (see Table 1), it can be understood that

there are more points in the parameter space corresponding to the “S1” solution under the assumption of flat distribution for the random values of the relevant parameters.

We illustrate the time-dependent CP asymmetries of the penguin-dominated modes in Fig. 9, taking values of $|B_{bs}^{L,R}|$, $\phi_{bs}^{L,R}$ and B_{dd}^R that are consistent with the constraints from $B_s - \bar{B}_s$ mixing and $B_d \rightarrow \pi K_S$ decays. As before, because of interference effects between the $B_d - \bar{B}_d$ mixing phase and ϕ_{bs}^L , the points in Fig. 9 are scattered away from the SM limits. Hence, for each decay mode there are once again always some points lying in the 1σ region. The allowed values for $|B_{bs}^{L,R}|$, $\phi_{bs}^{L,R}$ and B_{dd}^R due to the correlated analysis of the $B_s - \bar{B}_s$ mixing and the $B_d \rightarrow (\pi, \phi, \eta', \rho, \omega, f_0)K_S$ CP asymmetries are illustrated in Fig. 10. In Fig 11, as done before, we map the points in Fig. 10 back to the $q \cos \phi - q \sin \phi$ plane. It is straightforward to see that the points with $B_{dd}^R < -0.01$ are closer to the minima of the χ^2 fit of the $B \rightarrow \pi K$ and $B \rightarrow \pi\pi$ data, resulting in a better fit than that obtained in the SM limit.

4 Conclusions

In this paper, we have studied the constraints on extensions of the SM with family non-universal $U(1)'$ gauge symmetries which result from FCNC effects in the $b \rightarrow s$ transitions. Using a model-independent approach in which the main requirements are family universal charges for the first and second generations and small fermion mixing angles, we have performed a correlated analysis of this set of $\Delta B = 1, 2$ processes. Our results show that within this class of models, the possible anomalies in $B_s - \bar{B}_s$ mixing and the time-dependent CP asymmetries of the penguin-dominated $B_d \rightarrow (\pi, \phi, \eta', \rho, \omega, f_0)K_S$ decays can be accommodated in a consistent way.

Furthermore, the constraints from $B_s - \bar{B}_s$ mixing may have nontrivial implications not only for the hadronic decays, but also for the leptonic or semi-leptonic decays of the B_d mesons, as discussed in Section 2.1. As an example, recent results from BaBar [30] indicate an unexpectedly large isospin asymmetry in the low dilepton mass squared region for combined $B_d \rightarrow Kl^+l^-$ and $B_d \rightarrow K^*l^+l^-$. In addition, K^* longitudinal polarization and lepton forward-backward asymmetry are consistent with SM but seem to prefer a wrong-sign C_7 operator, suggestive of right-handed currents. We leave these interesting issues for future exploration.

Acknowledgments

We thank Cheng-Wei Chiang and Jonathan L. Rosner for useful discussions. Work at ANL is supported in part by the U.S. Department of Energy (DOE), Div. of HEP, Contract DE-AC02-06CH11357. Work at EFI is supported in part by the DOE through Grant No. DE-FG02-90ER40560. Work at the U. Wisconsin, Madison is supported by the DOE through Grant No. DE-FG02-95ER40896 and the Wisconsin Alumni Research Foundation. T.L. is also supported by the Fermi-McCormick Fellowship. The work of P.L. is supported by the IBM Einstein Fellowship and by NSF grant PHY-0503584.

Appendix A Operators of Effective Hamiltonians

A complete compilation of the relevant operators for the $b \rightarrow s$ transitions is given in the following:

Current-Current Operators:

$$Q_1 = (\bar{s}u)_{V-A} (\bar{u}b)_{V-A} \quad Q_2 = (\bar{s}_\alpha u_\beta)_{V-A} (\bar{u}_\beta b_\alpha)_{V-A} \quad (\text{A.1})$$

QCD-Penguin Operators:

$$Q_3 = (\bar{s}b)_{V-A} \sum_q (\bar{q}q)_{V-A} \quad Q_4 = (\bar{s}_\alpha b_\beta)_{V-A} \sum_q (\bar{q}_\beta q_\alpha)_{V-A} \quad (\text{A.2})$$

$$Q_5 = (\bar{s}b)_{V-A} \sum_q (\bar{q}q)_{V+A} \quad Q_6 = (\bar{s}_\alpha b_\beta)_{V-A} \sum_q (\bar{q}_\beta q_\alpha)_{V+A} \quad (\text{A.3})$$

$$\tilde{Q}_3 = (\bar{s}b)_{V+A} \sum_q (\bar{q}q)_{V+A} \quad \tilde{Q}_4 = (\bar{s}_\alpha b_\beta)_{V+A} \sum_q (\bar{q}_\beta q_\alpha)_{V+A} \quad (\text{A.4})$$

$$\tilde{Q}_5 = (\bar{s}b)_{V+A} \sum_q (\bar{q}q)_{V-A} \quad \tilde{Q}_6 = (\bar{s}_\alpha b_\beta)_{V+A} \sum_q (\bar{q}_\beta q_\alpha)_{V-A} \quad (\text{A.5})$$

Electroweak Penguin Operators:

$$Q_7 = \frac{3}{2} (\bar{s}b)_{V-A} \sum_q e_q (\bar{q}q)_{V+A} \quad Q_8 = \frac{3}{2} (\bar{s}_\alpha b_\beta)_{V-A} \sum_q e_q (\bar{q}_\beta q_\alpha)_{V+A} \quad (\text{A.6})$$

$$Q_9 = \frac{3}{2} (\bar{s}b)_{V-A} \sum_q e_q (\bar{q}q)_{V-A} \quad Q_{10} = \frac{3}{2} (\bar{s}_\alpha b_\beta)_{V-A} \sum_q e_q (\bar{q}_\beta q_\alpha)_{V-A} \quad (\text{A.7})$$

$$\tilde{Q}_7 = \frac{3}{2} (\bar{s}b)_{V+A} \sum_q e_q (\bar{q}q)_{V-A} \quad \tilde{Q}_8 = \frac{3}{2} (\bar{s}_\alpha b_\beta)_{V+A} \sum_q e_q (\bar{q}_\beta q_\alpha)_{V-A} \quad (\text{A.8})$$

$$\tilde{Q}_9 = \frac{3}{2} (\bar{s}b)_{V+A} \sum_q e_q (\bar{q}q)_{V+A} \quad \tilde{Q}_{10} = \frac{3}{2} (\bar{s}_\alpha b_\beta)_{V+A} \sum_q e_q (\bar{q}_\beta q_\alpha)_{V+A} \quad (\text{A.9})$$

Magnetic Penguin Operators:

$$Q_{7\gamma} = \frac{e}{8\pi^2} m_b \bar{s}_\alpha \sigma^{\mu\nu} (1 + \gamma_5) b_\alpha F_{\mu\nu} \quad Q_{8G} = \frac{g}{8\pi^2} m_b \bar{s}_\alpha \sigma^{\mu\nu} (1 + \gamma_5) T_{\alpha\beta}^a b_\beta G_{\mu\nu}^a \quad (\text{A.10})$$

Semi-Leptonic Operators:

$$\begin{aligned}
Q_{9V} &= (\bar{b}s)_{V-A}(\bar{l}l)_V & Q_{10A} &= (\bar{b}s)_{V-A}(\bar{l}l)_A \\
\tilde{Q}_{9V} &= (\bar{b}s)_{V+A}(\bar{l}l)_V & \tilde{Q}_{10A} &= (\bar{b}s)_{V+A}(\bar{l}l)_A
\end{aligned} \tag{A.11}$$

$B_s - \bar{B}_s$ Mixing Operators:

$$\begin{aligned}
Q_1^{B_s} &= (\bar{s}b)_{V-A}(\bar{s}b)_{V-A} & Q_2^{B_s} &= (\bar{s}_\alpha b_\beta)_{V-A}(\bar{s}_\beta b_\alpha)_{V-A} \\
\tilde{Q}_1^{B_s} &= (\bar{s}b)_{V+A}(\bar{s}b)_{V+A} & \tilde{Q}_2^{B_s} &= (\bar{s}_\alpha b_\beta)_{V+A}(\bar{s}_\beta b_\alpha)_{V+A} \\
Q_3^{B_s} = \tilde{Q}_3^{B_s} &= (\bar{s}b)_{V+A}(\bar{s}b)_{V-A} & Q_4^{B_s} = \tilde{Q}_4^{B_s} &= (\bar{s}_\alpha b_\beta)_{V+A}(\bar{s}_\beta b_\alpha)_{V-A}
\end{aligned} \tag{A.12}$$

where indices in color singlet currents have been suppressed for simplicity, and V and A refer to γ_μ and $\gamma_\mu\gamma_5$, respectively.

Appendix B Constraints of $\text{Br}(B_s \rightarrow \mu^+ \mu^-)$

For an order of magnitude estimate, one can temporarily ignore the effect of renormalization group running. Then the branching ratio of $B_s \rightarrow \mu^+ \mu^-$ is given by (also see [14])

$$\begin{aligned} \text{Br}(B_s \rightarrow \mu^+ \mu^-) &= \tau_{B_s} \frac{G_F^2}{4\pi} f_{B_s}^2 m_\mu^2 m_{B_s} \sqrt{1 - \frac{4m_\mu^2}{m_{B_s}^2} |V_{tb}^* V_{ts}|^2} \\ &\times \left\{ \left| \frac{\alpha}{2\pi \sin^2 \theta_W} Y \left(\frac{m_t^2}{M_W^2} \right) + 2 \frac{B_{bs}^L B_{\mu\mu}^L}{V_{tb}^* V_{ts}} \right|^2 \right. \\ &\left. + \left| 2 \frac{B_{bs}^L B_{\mu\mu}^R}{V_{tb}^* V_{ts}} \right|^2 + \left| 2 \frac{B_{bs}^R B_{\mu\mu}^L}{V_{tb}^* V_{ts}} \right|^2 + \left| 2 \frac{B_{bs}^R B_{\mu\mu}^R}{V_{tb}^* V_{ts}} \right|^2 \right\}. \end{aligned} \quad (\text{B.1})$$

Here τ_{B_s} is the lifetime of B_s meson, f_{B_s} is the corresponding decay constant, and $Y(m_t^2/M_W^2)$ in the SM part is defined in [31], with

$$Y(x) = \frac{x}{8} \left(\frac{4-x}{1-x} + \frac{3x}{(1-x)^2} \ln x \right). \quad (\text{B.2})$$

For $x = m_t^2/M_W^2$, we have $Y(x) \sim 1$. The present experimental exclusion limit at 2σ C.L. from a combination of CDF and D0 results is [32]

$$\text{Br}(B_s \rightarrow \mu^+ \mu^-) \leq 1.5 \times 10^{-7}, \quad (\text{B.3})$$

which thus give a constraint that

$$\left| 3 \times 10^{-3} + \frac{B_{bs}^L B_{\mu\mu}^L}{V_{tb}^* V_{ts}} \right|^2 + \left| \frac{B_{bs}^L B_{\mu\mu}^R}{V_{tb}^* V_{ts}} \right|^2 + \left| \frac{B_{bs}^R B_{\mu\mu}^L}{V_{tb}^* V_{ts}} \right|^2 + \left| \frac{B_{bs}^R B_{\mu\mu}^R}{V_{tb}^* V_{ts}} \right|^2 \lesssim 10^{-4}. \quad (\text{B.4})$$

In the LR and LL limits, we have $B_{bs}^L = B_{bs}^R \sim 10^{-3}$ and $B_{bs}^L \sim 10^{-3}$, $B_{bs}^R = 0$, respectively. For $(V_{L,R} \tilde{\epsilon}^{L,R} V_{L,R})_{22} \sim \mathcal{O}(1)$ and $g_1 M_{Z'}/(g_2 M_Z) \sim 10 - 100$ (a parameter region favored by the correlated analysis of the anomalies in $B_s \rightarrow \bar{B}_s$ mixing and time-dependent CP asymmetries of penguin-dominated B_d meson decays; for details, see the last paragraph of subsection 3.1), this means that the NP contribution is comparable with the SM one. The experimental bound therefore can be easily satisfied. This conclusion also applies to the general case.

Appendix C Parameters

The parameters used in our numerical analysis are summarized below:

Masses, Decay Constants, Hadronic Form Factors, and Lifetimes:

$$\begin{aligned}
M_{\pi^\pm} &= 0.139 \text{ GeV}, & M_{\pi^0} &= 0.135 \text{ GeV}, \\
M_K &= 0.498 \text{ GeV}, & M_B &= 5.279 \text{ GeV}, \\
M_\phi &= 1.02 \text{ GeV}, & M_\psi &= 2.097 \text{ GeV}, \\
M_{\eta'} &= 0.958 \text{ GeV}, & M_\omega &= 0.783 \text{ GeV}, \\
M_\rho &= 0.776 \text{ GeV}, & M_\eta &= 0.548 \text{ GeV}, \\
M_{f^0} &= 0.980 \text{ GeV}, \\
X_\eta &= 0.57, & Y_\eta &= 0.82, \\
m_u(\mu = 4.2 \text{ GeV}) &= 1.86 \text{ MeV}, & m_d(\mu = 4.2 \text{ GeV}) &= 4.22 \text{ MeV}, \\
m_s(\mu = 4.2 \text{ GeV}) &= 80 \text{ MeV}, & m_c(\mu = 4.2 \text{ GeV}) &= 0.901 \text{ GeV}, \\
m_b(\mu = 4.2 \text{ GeV}) &= 4.2 \text{ GeV}, & m_t(\mu = M_Z) &= 171.7 \text{ GeV}, \\
f_\phi &= 237 \text{ MeV}, & f_B &= 190 \text{ MeV}, \\
f_\pi &= 130 \text{ MeV}, & f_K &= 160 \text{ MeV}, \\
f_\psi &= 410 \text{ MeV}, & f_\omega &= 200 \text{ MeV}, \\
f_\rho &= 209 \text{ MeV}, & f_{f^0} &= 180 \text{ MeV}, \\
F_0^{B\pi}(0) &= 0.330, & F_0^{BK}(0) &= 0.379, \\
F_1^{BK}(0) &= 0.379, & A_0^{B\omega}(0) &= 0.280, \\
F_0^{Bf}(0) &= 0.250, & F_0^{fK}(0) &= 0.030, \\
A_0^{B\rho} &= 0.280, & f_{B_s} \sqrt{\hat{B}_{B_s}} &= 0.262 \\
\tau_{B^0} &= 1.530 \text{ ps}, & \tau_{B^-} &= 1.65 \text{ ps}, \\
M_{B_s} &= 5.37 \text{ GeV}, & \tau_{B_s} &= 1.47 \text{ ps},
\end{aligned}$$

QCD and EW Parameters:

$$\begin{aligned}
G_F &= 1.16639 \times 10^{-5} \text{ GeV}^{-2}, & \Lambda_{\overline{MS}}^{(5)} &= 225 \text{ MeV}, \\
M_W &= 80.42 \text{ GeV}, & \sin^2 \theta_W &= 0.23, \\
\eta_{2B} &= 0.55, & J_5 &= 1.627, \\
\alpha_s(M_Z) &= 0.118, & \alpha_{em} &= 1/128, \\
\lambda &= 0.2252, & A &= 0.8117, \\
\bar{\rho} &= 0.145, & \bar{\eta} &= 0.339, \\
R_b &= \sqrt{\rho^2 + \eta^2} = 0.378.
\end{aligned}$$

Hadronic Parameters from Lattice Calculations:

$$f_{B_s} \sqrt{\hat{B}_{B_s}} = 0.262.$$

References

- [1] J. H. Christenson, J. W. Cronin, V. L. Fitch and R. Turlay, Phys. Rev. Lett. **13**, 138 (1964).
- [2] N. Cabibbo, Phys. Rev. Lett. **10**, 531 (1963).
- [3] M. Kobayashi and T. Maskawa, Prog. Theor. Phys. **49**, 652 (1973).
- [4] C. Amsler *et al.* [Particle Data Group], Phys. Lett. B **667**, 1 (2008); <http://pdg.lbl.gov/>.
- [5] M. B. Gavela *et al.*, Mod. Phys. Lett. A **9**, 795 (1994) [arXiv:hep-ph/9312215], Nucl. Phys. B **430**, 345 (1994) [arXiv:hep-ph/9406288], Nucl. Phys. B **430**, 382 (1994) [arXiv:hep-ph/9406289]; P. Huet and E. Sather, Phys. Rev. D **51**, 379 (1995) [arXiv:hep-ph/9404302]; G. R. Farrar and M. E. Shaposhnikov, Phys. Rev. D **50**, 774 (1994) [arXiv:hep-ph/9305275].
- [6] M. Bona *et al.* [UTfit Collaboration], arXiv:0803.0659 [hep-ph]; M. Bona *et al.*, arXiv:0906.0953 [hep-ph].
- [7] T. Aaltonen *et al.* [CDF Collaboration], Phys. Rev. Lett. **100**, 161802 (2008) arXiv:0712.2397 [hep-ex].
- [8] V. M. Abazov *et al.* [D0 Collaboration], Phys. Rev. Lett. **101**, 241801 (2008) arXiv:0802.2255 [hep-ex].
- [9] C. Tarantino, Nuovo Cim. **123B**, 437 (2008) arXiv:0805.0698 [hep-ph].
- [10] E. Barberio *et al.*, “Averages of b-hadron and c-hadron Properties at the End of 2007,” arXiv:0808.1297 [hep-ex]; <http://www.slac.stanford.edu/xorg/hfag/>.
- [11] B. Dutta and Y. Mimura, Phys. Rev. D **78**, 071702 (2008) arXiv:0805.2988 [hep-ph]; M. Blanke, A. Buras, S. Recksiegel and C. Tarantino, arXiv:0805.4393 [hep-ph]; A. Soni, A. Alok, A. Giri, R. Mohanta and S. Nandi, arXiv:0807.1971 [hep-ph]; M. Blanke, A. J. Buras, B. Duling, S. Gori and A. Weiler, JHEP **0903** (2009) 001 arXiv:0809.1073 [hep-ph].
- [12] P. Langacker, arXiv:0801.1345 [hep-ph].
- [13] P. Langacker and M. Plumacher, Phys. Rev. D **62**, 013006 (2000) [arXiv:hep-ph/0001204].
- [14] V. Barger, L. L. Everett, J. Jiang, P. G. Langacker, T. Liu and C. E. M. Wagner, arXiv:0902.4507 [hep-ph].
- [15] V. Barger, C. W. Chiang, P. Langacker and H. S. Lee, Phys. Lett. B **580**, 186 (2004) [arXiv:hep-ph/0310073].

- [16] Phys. Lett. B **598**, 218 (2004) [arXiv:hep-ph/0406126]; V. Barger, C. W. Chiang, J. Jiang and P. Langacker, Phys. Lett. B **596**, 229 (2004) [arXiv:hep-ph/0405108]; S. Baek, J. H. Jeon and C. S. Kim, Phys. Lett. B **664**, 84 (2008) arXiv:0803.0062 [hep-ph]; X. G. He and G. Valencia, Phys. Rev. D **74**, 013011 (2006) [arXiv:hep-ph/0605202]; K. Cheung, C. W. Chiang, N. G. Deshpande and J. Jiang, Phys. Lett. B **652**, 285 (2007) [arXiv:hep-ph/0604223]; R. Mohanta and A. K. Giri, arXiv:0812.1842 [hep-ph]. Q. Chang, X. Q. Li and Y. D. Yang, arXiv:0903.0275 [hep-ph].
- [17] A. J. Buras, R. Fleischer, S. Recksiegel and F. Schwab, Phys. Rev. Lett. **92**, 101804 (2004) [arXiv:hep-ph/0312259]; Nucl. Phys. B **697**, 133 (2004) [arXiv:hep-ph/0402112].
- [18] G. Buchalla, A. J. Buras and M. E. Lautenbacher, Rev. Mod. Phys. **68**, 1125 (1996) [arXiv:hep-ph/9512380].
- [19] R. Fleischer, S. Jager, D. Pirjol and J. Zupan, Phys. Rev. D **78**, 111501 (2008) arXiv:0806.2900 [hep-ph].
- [20] M. Gronau and J. L. Rosner, Phys. Lett. B **666**, 467 (2008) arXiv:0807.3080 [hep-ph].
- [21] C. W. Chiang, M. Gronau, J. L. Rosner and D. A. Suprun, Phys. Rev. D **70**, 034020 (2004) [arXiv:hep-ph/0404073].
- [22] S. Baek, C. W. Chiang and D. London, arXiv:0903.3086 [hep-ph].
- [23] M. Ciuchini, E. Franco, G. Martinelli, M. Pierini and L. Silvestrini, Phys. Lett. B **674**, 197 (2009) arXiv:0811.0341 [hep-ph].
- [24] A. Ali, G. Kramer and C. D. Lu, Phys. Rev. D **58**, 094009 (1998) [arXiv:hep-ph/9804363].
- [25] U. Nierste, Nucl. Phys. Proc. Suppl. **170**, 135 (2007) [arXiv:hep-ph/0612310].
- [26] E. Barberio *et al.* [Heavy Flavor Averaging Group (HFAG) Collaboration], arXiv:0704.3575 [hep-ex].
- [27] M. Wirbel, B. Stech and M. Bauer, Z. Phys. C **29**, 637 (1985); M. Bauer, B. Stech and M. Wirbel, Z. Phys. C **34**, 103 (1987); J. G. Korner and G. A. Schuler, Z. Phys. C **38**, 511 (1988) [Erratum-ibid. C **41**, 690 (1988)]; M. Bauer and M. Wirbel, Z. Phys. C **42**, 671 (1989).
- [28] http://ckmfitter.in2p3.fr/plots_Summer08/ckmEval_results.html.
- [29] M. S. Carena, A. Daleo, B. A. Dobrescu and T. M. P. Tait, Phys. Rev. D **70**, 093009 (2004) [arXiv:hep-ph/0408098].

- [30] B. Aubert *et al.* [BABAR Collaboration], Phys. Rev. Lett. **102**, 091803 (2009) arXiv:0807.4119 [hep-ex]; K. T. Flood [Babar Collaboration], arXiv:0810.0837 [hep-ex].
- [31] G. Buchalla and A. J. Buras, Nucl. Phys. B **400**, 225 (1993).
- [32] R. Bernhard *et al.* [CDF Collaboration and D0 Collaboration], arXiv:hep-ex/0508058.

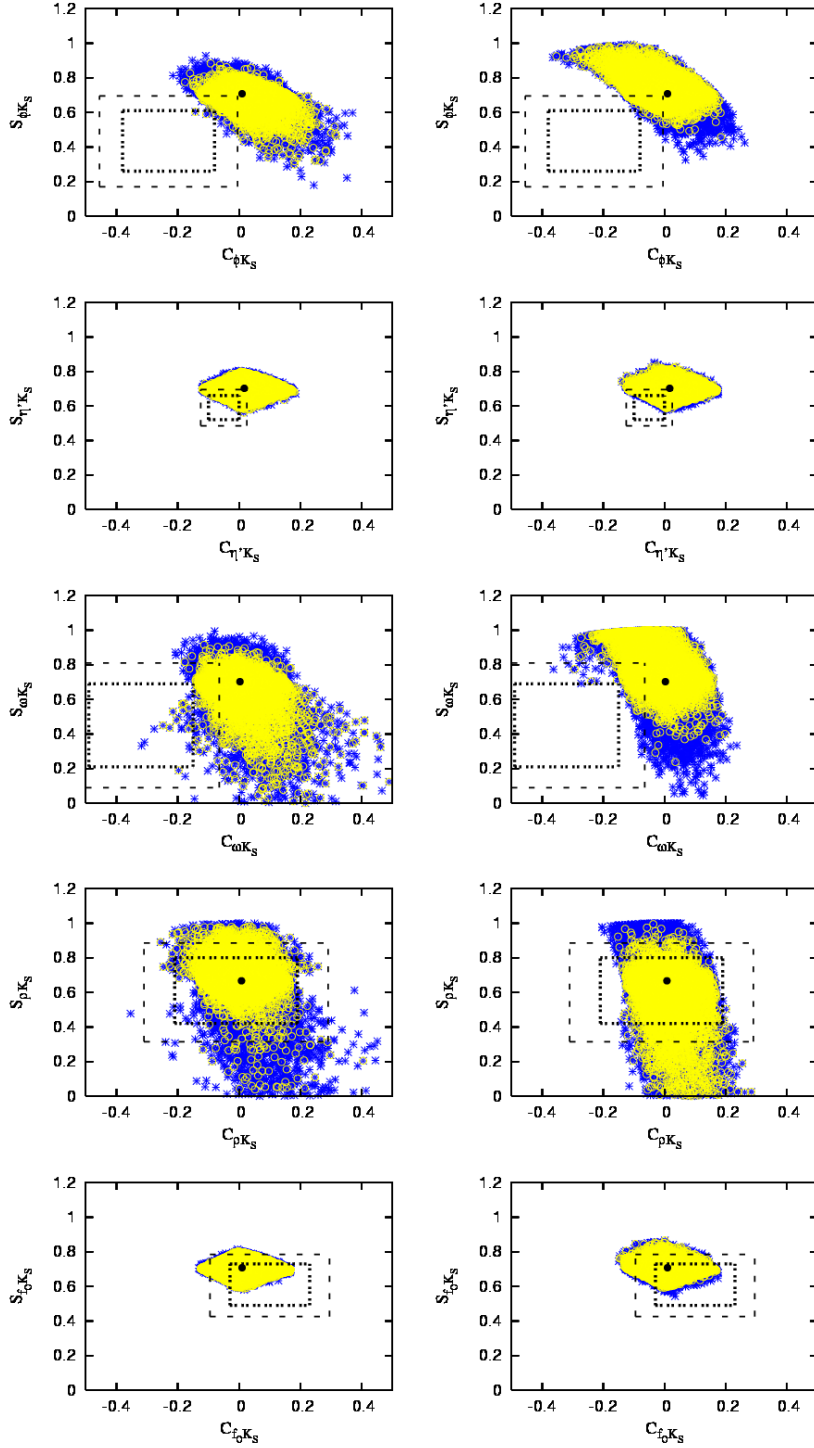


Figure 4: With B_{bs}^L and B_{dd}^R constrained by $B_s - \bar{B}_s$ mixing and $B_d \rightarrow \pi K_S$, the NP contributions to $\mathcal{C}_{(\phi,\eta',\rho,\omega,f_0)K_S}$ and $\mathcal{S}_{(\phi,\eta',\rho,\omega,f_0)K_S}$ are shown. The left (right) panels are the LR (LL) limits. The colors specify the C.L. that their inverse image points represent in Figs. 1 and 2 (yellow for 1σ C.L. and blue for 2σ and 1.7σ C.L.). The boxes specify the experimentally allowed regions at 1σ and 1.7σ , and the dark point denotes the SM limit.

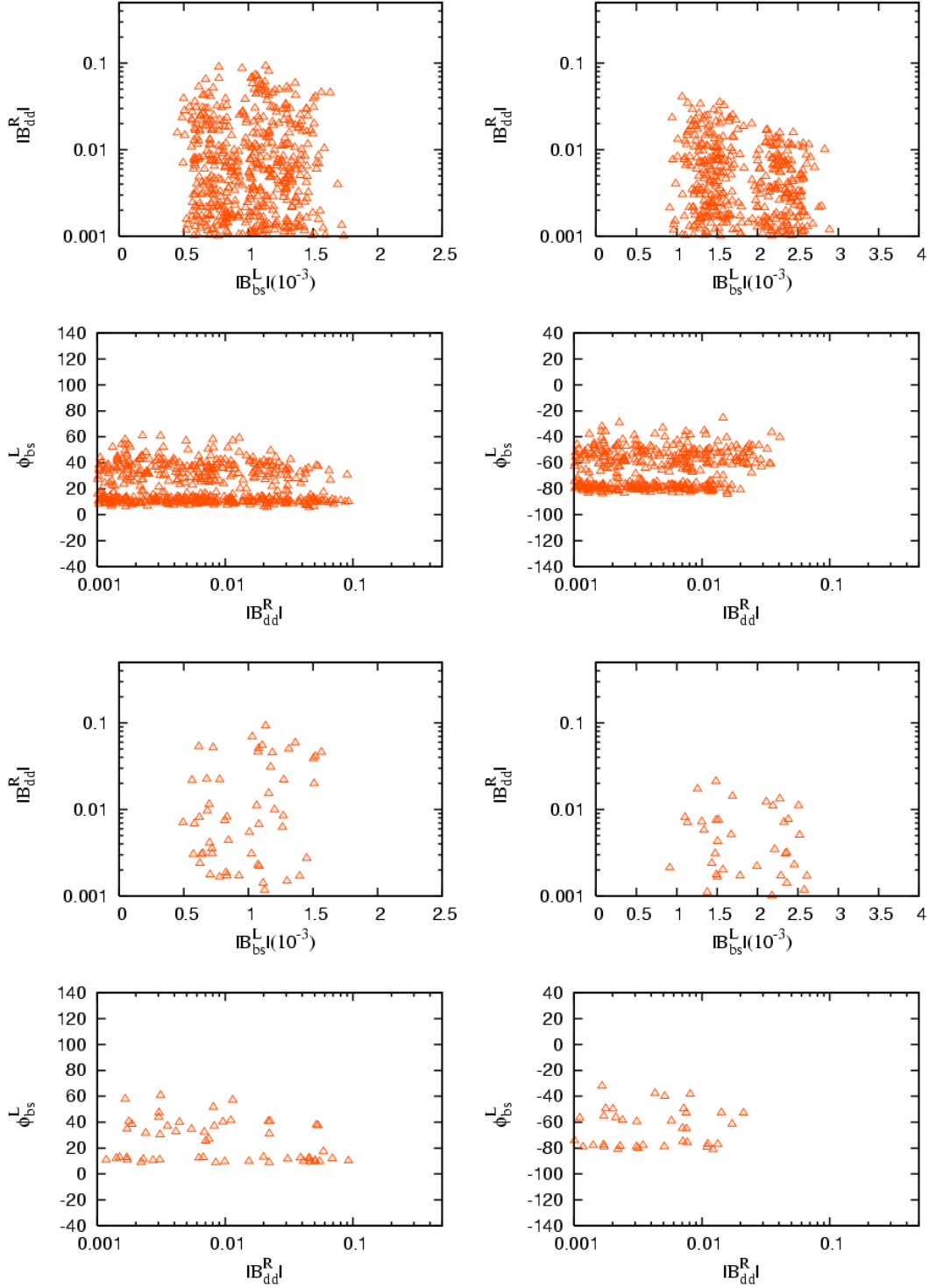


Figure 5: The allowed $|B_{bs}^L|$, $\phi_{bs}^L[^\circ]$ and B_{dd}^R are shown. They are constrained from $B_s - \bar{B}_s$ mixing (at 2σ C.L.) and the χ^2 fit of the $B \rightarrow \pi K$ (and $B \rightarrow \pi\pi$) data (at 1σ C.L.), then selected by $\mathcal{C}_{(\phi,\eta',\rho,\omega,f_0)K_S}$, $\mathcal{S}_{(\phi,\eta',\rho,\omega,f_0)K_S}$ (at 1.7σ C.L. for the first four panels and 1.5σ C.L. for the others). The left (right) panels are the LR (LL) limits.

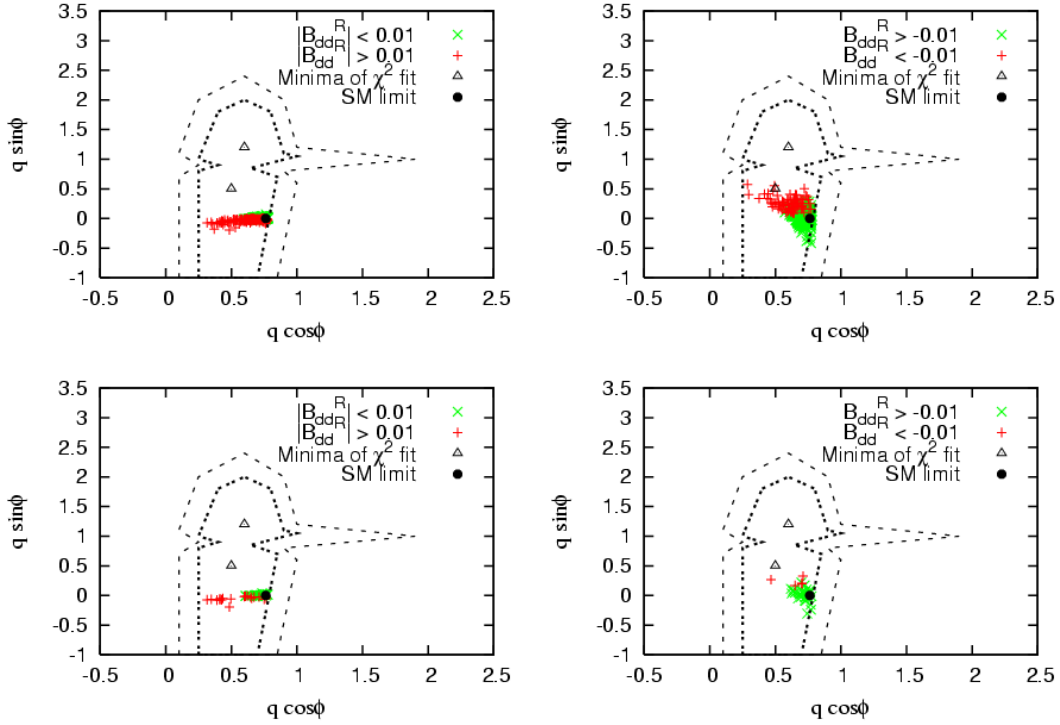


Figure 6: The points in Fig. 5 are inversely mapped to the $q \cos \phi - q \sin \phi$ plane. The panels in the first row correspond to a parameter selection from $\mathcal{C}_{(\phi, \eta', \rho, \omega, f_0)K_S}$, $\mathcal{S}_{(\phi, \eta', \rho, \omega, f_0)K_S}$ at 1.7σ C.L. in Fig. 5, and those in the second row at 1.5σ C.L.. The left (right) panels are the LR (LL) limits.

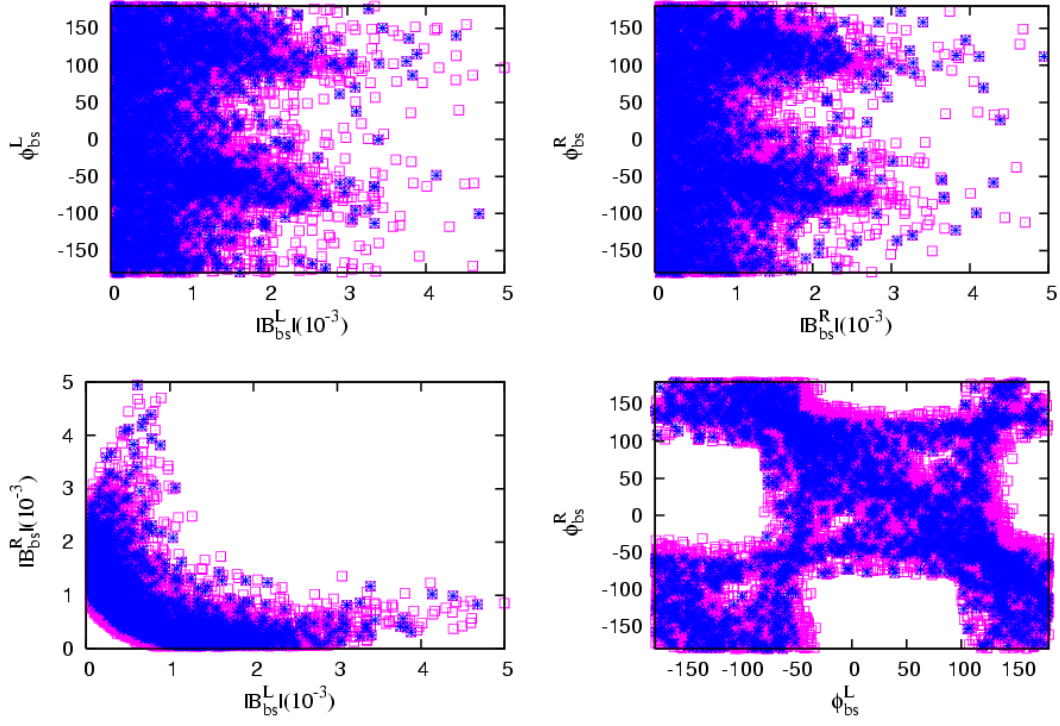


Figure 7: The distributions of $|B_{bs}^{L,R}|$ and $\phi_{bs}^{L,R}$ resulting from $B_s - \bar{B}_s$ mixing constraints are shown. The blue and purple points can be mapped to the experimentally allowed $\{C_{B_s}, \phi_{B_s}^{\text{NP}}\}$ regions with 1σ and 2σ C.L., respectively. Here we did not distinct S1 and S2 solutions any more.

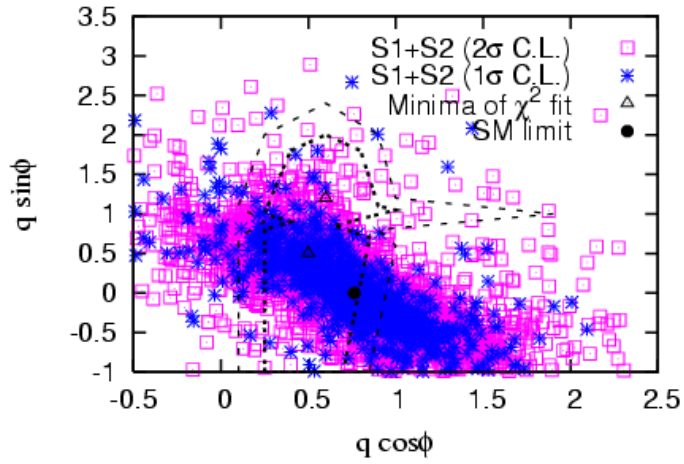


Figure 8: The constraints on B_{dd}^R from $qe^{i\phi}$ are illustrated. The points of $|B_{bs}^{L,R}|$ and $\phi_{bs}^{L,R}$ from Fig. 7 are randomly combined with the scattered points of B_{dd}^R ($10^{-3} < |B_{dd}^R| < 10^{-1}$) and then mapped to the $q \cos \phi - q \sin \phi$ plane according to Eq. (2.48). The colors of the points in this plane indicate the C.L. that their inverse images represent in Fig. 7.

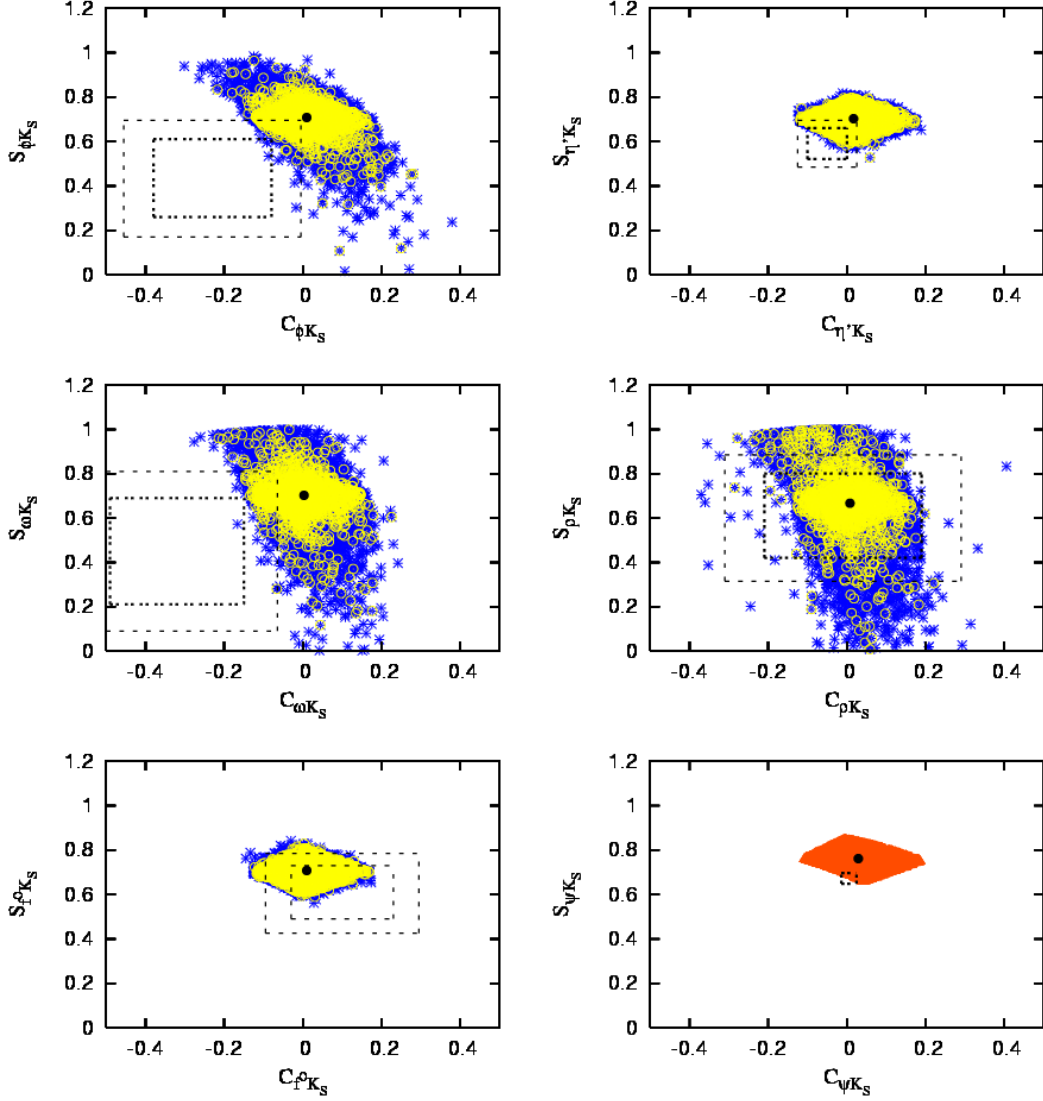


Figure 9: With the values of $|B_{bs}^{L,R}|$, $\phi_{bs}^{L,R}$ and B_{dd}^R fixed by $B_s - \bar{B}_s$ mixing and $B_d \rightarrow \pi K_S$ decay, the NP contributions to $\mathcal{C}_{(\phi,\eta',\rho,\omega,f_0)K_S}$ and $\mathcal{S}_{(\phi,\eta',\rho,\omega,f_0)K_S}$ are illustrated in the first five panels. The colors of the points specify the C.L. that their inverse image points represent in Fig. 7 and Fig. 8 (yellow denotes 1σ C.L. in both and blue denotes 2σ and 1.7σ C.L., separately). In the last panel, the CP asymmetries of the charmed $B_d \rightarrow \psi K_S$ decay are presented ($|V_{ub}| = 3.51 \times 10^{-3}$ [28]). For each, the two boxes specify the 1σ and 1.7σ allowed regions (except for the last panel, where only the 1σ box is given), and the dark point denotes the SM limit.

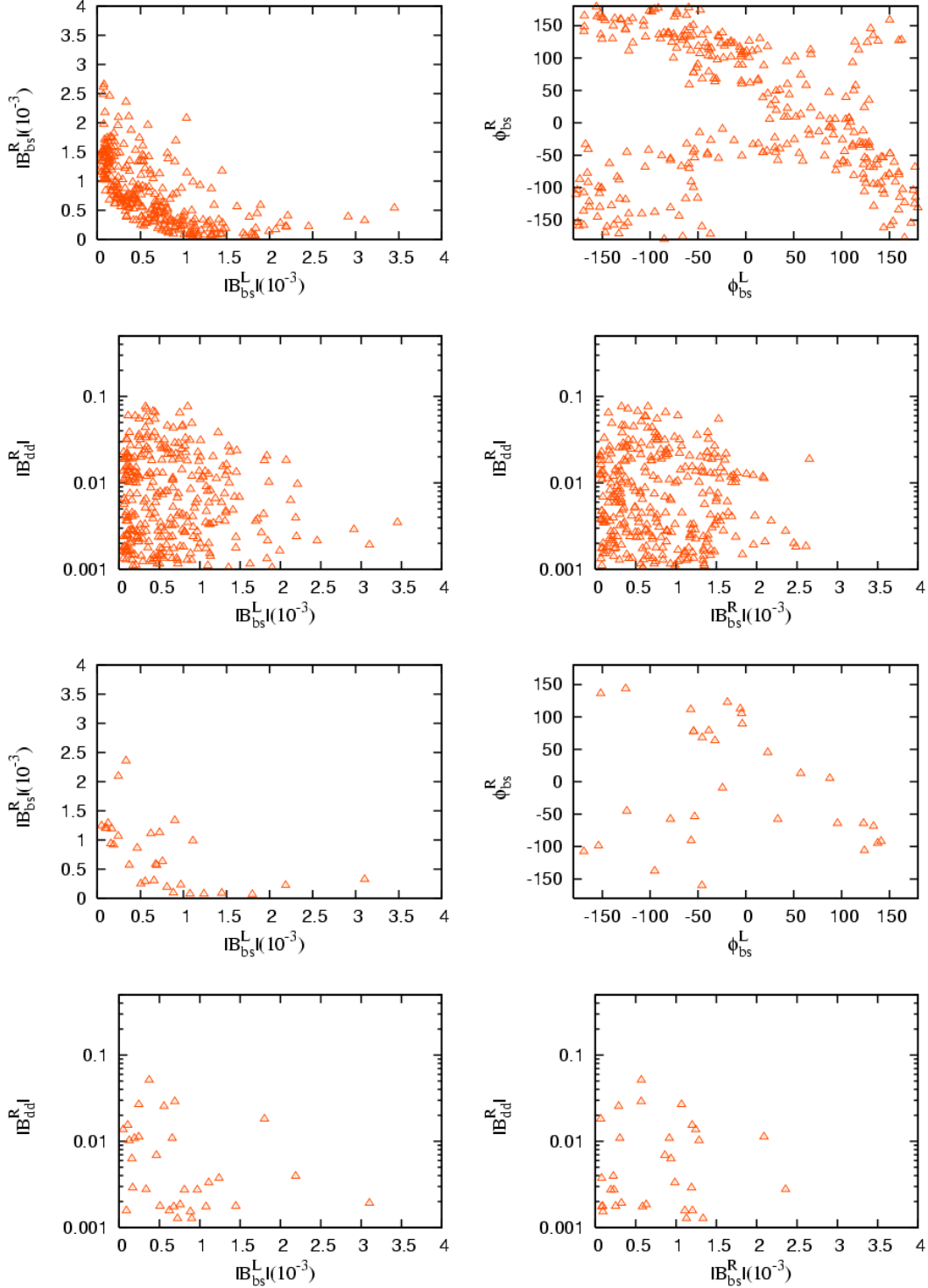


Figure 10: The distributions of $|B_{bs}^{L,R}|$, $\phi_{bs}^{L,R}$ and B_{dd}^R are shown. The values are constrained by $B_s - \bar{B}_s$ mixing (2σ C.L.) and the χ^2 fit of the $B \rightarrow \pi K$ (and $B \rightarrow \pi\pi$) data (1σ C.L.), then selected by $\mathcal{C}_{(\phi,\eta',\rho,\omega,f_0)K_S}$, $\mathcal{S}_{(\phi,\eta',\rho,\omega,f_0)K_S}$ (1.7σ C.L. for the first four panels and 1.5σ C.L. for the rest).

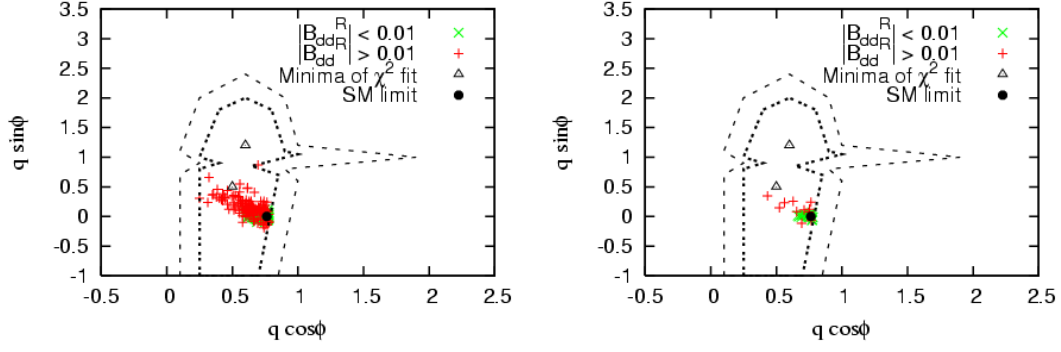


Figure 11: The points in Fig. 11 are inversely mapped to the $q \cos \phi - q \sin \phi$ plane. The parameter selection from $\mathcal{C}_{(\phi, \eta', \rho, \omega, f_0)K_S}$, $\mathcal{S}_{(\phi, \eta', \rho, \omega, f_0)K_S}$ is shown at 1.7σ C.L. in Fig. 11 the left panel, and at 1.5σ C.L. in the right panel.